AFRL-HE-WP-TR-2002-0172

UNITED STATES AIR FORCE
RESEARCH LABORATORY

SUMMARY STATISTICS AND HGU-55/P
FEATURE ENVELOPES FOR THE
1990 USAF ANTHROPOMETRIC SURVEY

Jennifer J. Whitestone
Gregory F. Zehner

HUMAN EFFECTIVENESS DIRECTORATE
CREW SYSTEM INTERFACE DIVISION
WRIGHT-PATTERSON AFB OH 45433-7022

Daniel J. Mountjoy
Sherri U. Blackwell
Mary E. Gross
Deepa Naishadham

SYTRONICS, INC.
4433 DAYTON-XENIA RD., BLDG. 1
DAYTON OH 45432

APRIL 1998

INTERIM REPORT FOR THE PERIOD MARCH 1990 TO MARCH 1991

20030321 020

Human Effectiveness Directorate
Crew System Interface Division
2255 H Street
Wright-Patterson AFB OH 45433-7022

NOTICES

When US Government drawings, specifications, or other data are used for any purpose other than a definitely related Government procurement operation, the Government thereby incurs no responsibility nor any obligation whatsoever, and the fact that the Government may have formulated, furnished, or in any way supplied the said drawings, specifications, or other data, is not to be regarded by implication or otherwise, as in any manner licensing the holder or any other person or corporation, or conveying any rights or permission to manufacture, use, or sell any patented invention that may in any way be related thereto.

Please do not request copies of this report from the Air Force Research Laboratory. Additional copies may be purchased from:

Federal Government agencies and their contractors registered with the Defense Technical Information Center should direct requests for copies of this report to:
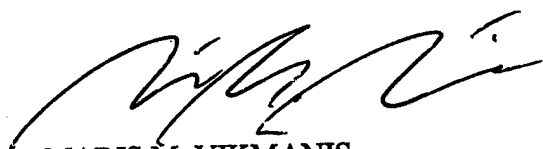
TECHNICAL REVIEW AND APPROVAL

AFRL-HE-WP-TR-2002-0172

This report has been reviewed by the Office of Public Affairs (PA) and is releasable to the National Technical Information Service (NTIS). At NTIS, it will be available to the general public.

The voluntary informed consent of the subjects used in this research was obtained as required by Air Force Instruction 40-402.

This technical report has been reviewed and is approved for publication.

FOR THE COMMANDER

MARIS M. VIKMANIS
Chief, Crew System Interface Division
Air Force Research Laboratory

REPORT DOCUMENTATION PAGE

Public reporting burden for this collection of information is estimated to average 1 hour per response, including the time for reviewing the collection of information. Send comments regarding this burden estimate or any other aspect of this collection of information, including suggestions for reducing this burden, to Washington Headquarters Services, Directorate for Information Operations and Reports, 1215 Jefferson Davis Highway, Suite 1204, Arlington, VA 22202-4302, and to the Office of Management and Budget, Paperwork Reduction Project (0704-0188), Washington, DC 20503.

| 1. AGENCY USE ONLY (Leave Blank) | 2. REPORT DATE
April 1998 | 3. REPORT TYPE AND DATES COVERED
Interim Report,   March 1990 to   March 1991 |
|---|---|---|

4. TITLE AND SUBTITLE

Summary Statistics and HGU-55/P Feature Envelopes for the

1990 USAF Anthropometric Survey

5. FUNDING NUMBERS

C   F41624-93-C-6001
PE 62202F
PR 7184
TA 08
WU 60

6. AUTHOR(S)

Whitestone, Jennifer J., Zehner, Gregory F., Mountjoy, Daniel J.*, Blackwell, Sherri U.*, Gross, Mary E.*, Naishadham, Deepa*

7. PERFORMING ORGANIZATION NAME(S) AND ADDRESS(ES)
*Sytronics, Inc.

4433 Dayton-Xenia Rd, Bldg 1

Dayton, OH 45432

**8. PERFORMING ORGANIZATION
REPORT NUMBER**

9. SPONSORING/MONITORING AGENCY NAME(S) AND ADDRESS(ES)
Air Force Research Laboratory
Human Effectiveness Directorate
Crew System Interface Division
Air Force Materiel Command
Wright-Patterson AFB OH 45433-7022

**10. SPONSORING/MONITORING
AGENCY REPORT NUMBER**

AFRL-HE-WP-TR-2002-0172

11. SUPPLEMENTARY NOTES

12a. DISTRIBUTION/AVAILABILITY STATEMENT

Approved for public release; distribution is unlimited

12b. DISTRIBUTION CODE

13. ABSTRACT (Maximum 200 words)

This report describes an anthropometric survey of 365 USAF flyers conducted in 1990 at four military bases, including Ellsworth AFB, South Dakota; Randolph AFB, Texas; Eglin AFB, Florida; and Hurlburt Field, Florida. The survey included both traditional measurement data on the whole body, such as stature and thumbtip-reach, and three-dimensional (3-D) anthropometry acquired on the head and face. Surface scans of the flyers with and without their helmets were acquired to provide a database for cranio-facial design applications. The scans were used to establish feature envelopes for the HGU-55/P helmet. This report documents the 3-D relationship between anatomical features and equipment for a population of USAF flyers wearing the HGU-55/P helmet.

14. SUBJECT TERMS

| anthropometry | three-dimensional | feature envelopes |
| helmet | cranio-facial | survey |

15. NUMBER OF PAGES
90

16. PRICE CODE

| 17. SECURITY CLASSIFICATION
OF REPORT
Unclassified | 18. SECURITY CLASSIFICATION
OF THIS PAGE
Unclassified | 19. SECURITY CLASSIFICATION
OF ABSTRACT
Unclassified | 20. LIMITATION OF ABSTRACT
Unlimited |
|---|---|---|---|

THIS PAGE INTENTIONALLY LEFT BLANK

ABSTRACT

This report describes an anthropometric survey of 365 USAF flyers conducted in 1990 at four military bases, including Ellsworth AFB, South Dakota; Randolph AFB, Texas; Eglin AFB, Florida; and Hurlburt Field, Florida. The survey included both traditional measurement data on the whole body, such as stature and thumbtip-reach, and three-dimensional (3-D) anthropometry acquired on the head and face. Surface scans of the flyers with and without their helmets were acquired to provide a database for cranio-facial design applications. The scans were used to establish feature envelopes for the HGU-55/P helmet. This report documents the 3-D relationship between anatomical features and equipment for a population of USAF flyers wearing the HGU-55/P helmet.

PREFACE

TABLE OF CONTENTS

THIS PAGE INTENTIONALLY LEFT BLANK

1.0 INTRODUCTION

1.1 Purpose of Survey

This technical report documents an anthropometric survey and subsequent analysis of data collected on USAF aircrew at the following sites: Ellsworth AFB, South Dakota; Randolph AFB, Texas; Eglin AFB, Florida; and Hurlburt Field, Florida. Survey data included traditional anthropometric measurements on the head and whole body, three-dimensional (3-D) anthropometry of the head and face in the form of surface scan data, fit geometries of the HGU-55/P helmet (also surface scan data), and demographic and biographic information on 365 USAF subjects. These data have been used to establish a database of USAF flyers anthropometry available through the Computerized Anthropometric Research and Design (CARD) Laboratory, Human Engineering Division, Armstrong Laboratory located at Wright-Patterson AFB, Ohio. The 3-D surface data acquired during the survey include scans of bare heads (unencumbered) and scans of pilots wearing their personal helmets (encumbered). The combination of these images was used to establish the HGU-55/P feature envelopes.

This report contains the following information:

Section 1.2 -- the need for 3-D anthropometry,

Section 2.1 -- specific aims of this survey,

Section 2.2 -- survey population description,

Section 2.3 -- survey data collection methods, .

Section 2.4 -- summary statistics of survey demographics and anthropometry,

Section 3.1 -- history and definition of feature envelopes,

Section 3.2 -- generating feature envelopes for a helmet-mounted system,

Section 4.1 -- feature envelopes for the HGU-55/P helmet system,

Section 4.2 -- description of recommendations for using feature envelopes.

1.2 Three-Dimensional (3-D) Anthropometry

Traditional anthropometric measurements, such as the lengths, breadths, and circumferences of various body segments, have been used for years in the design of clothing and personal protective equipment. However, the poor fit offered by many of these items suggests that these types of measurements do not provide enough information to optimize the design. The range of anthropometric fit and, in this case, the interface geometries between the head and the helmet, are required to obtain sufficient information for appropriate design criteria.

1

Historically, when face forms or headforms were created for helmet or oxygen mask designers, distances between anatomical landmarks were provided to a sculptor, who used this information to build a representative form. However, the shape of the form between data points was filled in by the sculptor's artistic impressions. Even when working with as many as 42 landmarks on the head and face, as shown in Figure 1, this leaves a lot to the artist's imagination. At one time, this was the only way to provide designers with human shape information.
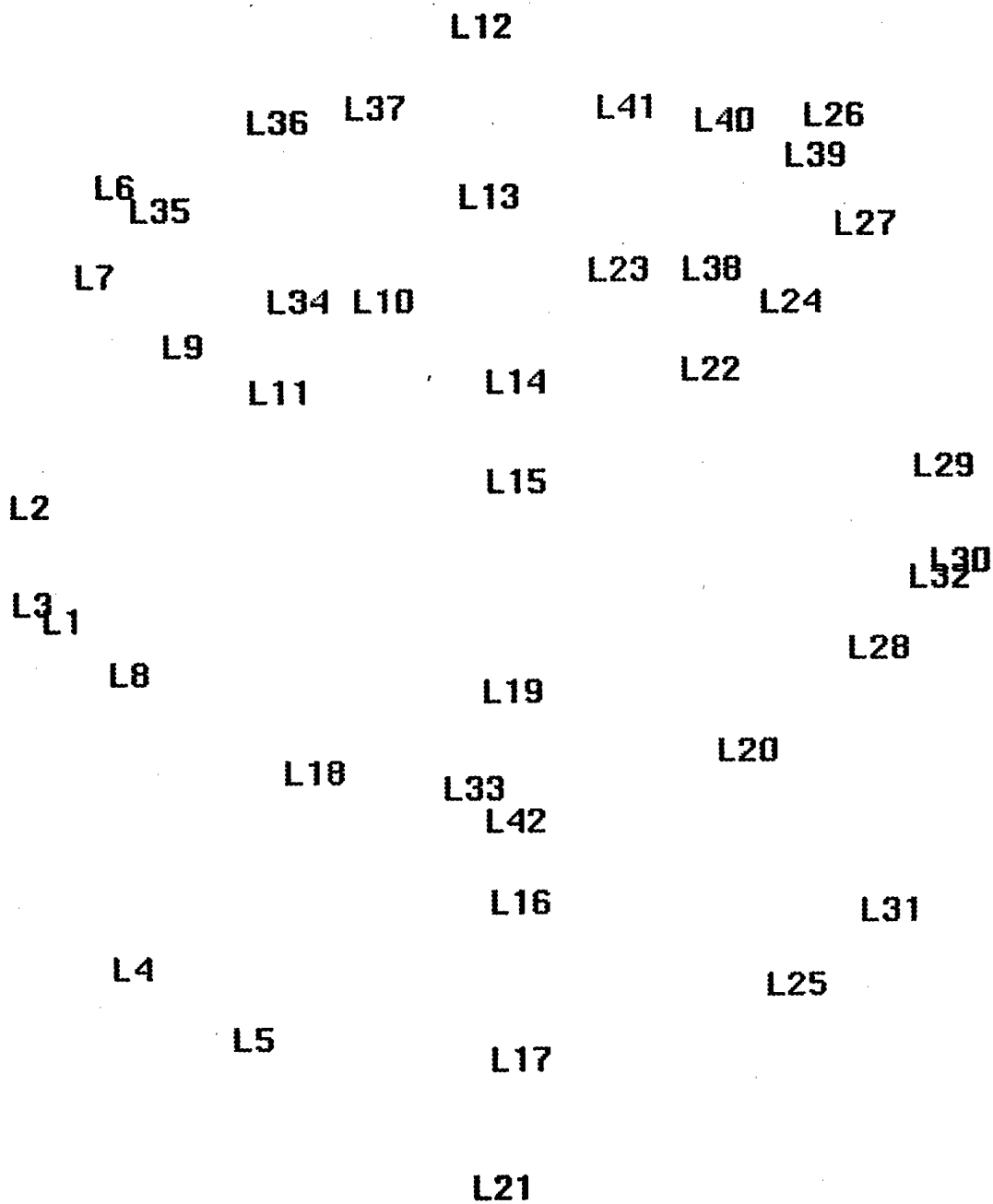
Figure 1

Illustration of 42 anatomical landmarks located on the head and face

3

In the 1980's, with the advent of commercially available, three-dimensional surface scanning technologies, came the ability to capture an accurate three-dimensional representation of an individual's head and face. In 1986, the CARD Lab purchased a Cyberware 4020-PS 3-D Digitizer. This scanner collects over 131,000 three-dimensional data points in approximately seventeen seconds (Hoffmeister, Pohlenz, Addleman, Kasic, & Robinette, 1996). Resolution varies depending on the radius of the object being scanned, but is approximately 1.5 millimeters vertically and 1 millimeter horizontally over the entire head and face. Figure 2 is an image of surface data captured using the Cyberware scanning system. During the scan, a Helium-neon laser is spread into a vertical plane of light which illuminates a contour on the object. A Charge Coupled Device (CCD) camera then views this contour from an angle, and using triangulation principles, the scanner software calculates distances from the scanner's center of rotation to 256 points along the profile. The scanner rotates about the object and digitizes a total of 512 profiles.
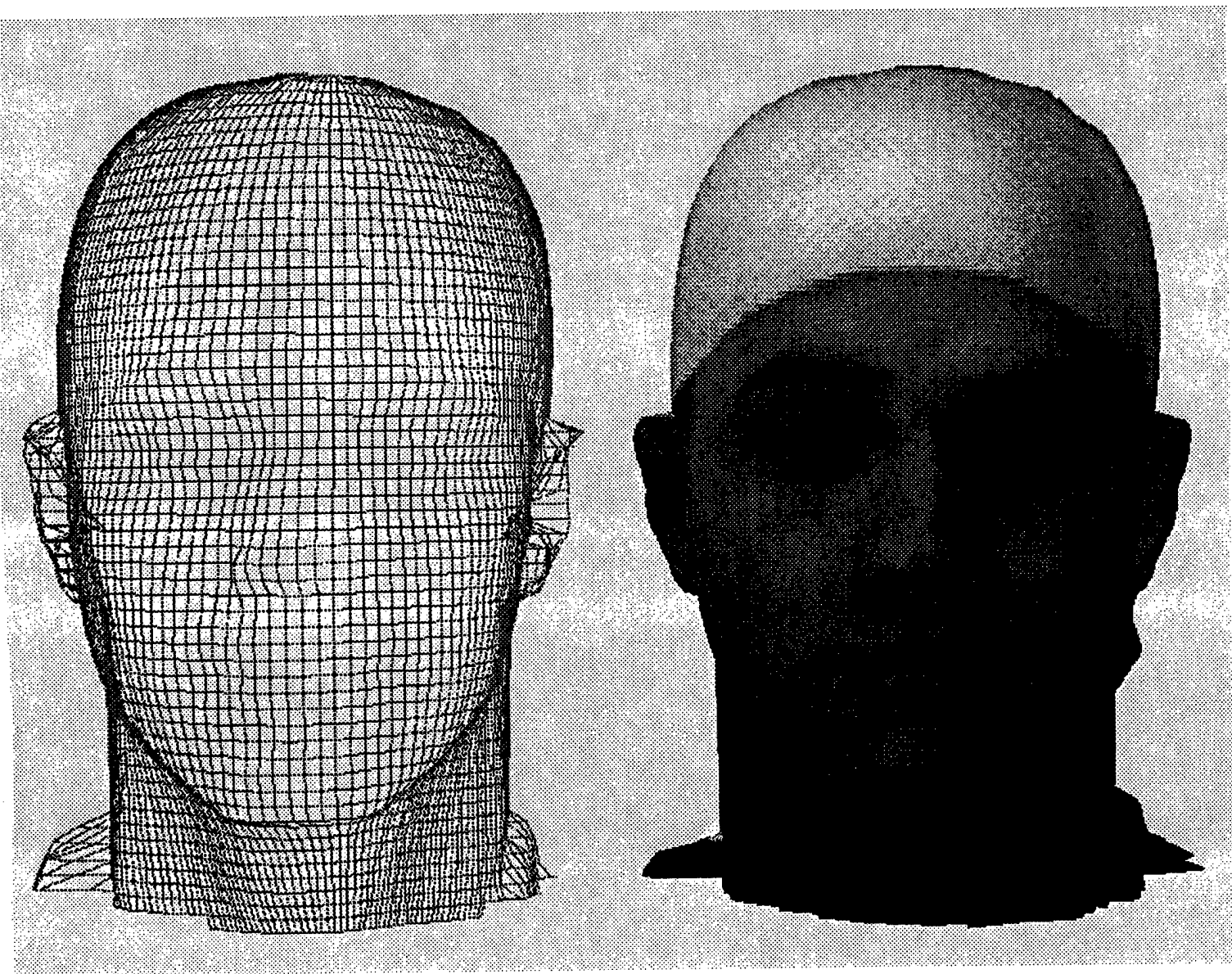
Figure 2

Cyberware scan data of a subject (wireframe and surface)

Once captured, the three-dimensional data may be imported to an application software package such as Computer-Aided Design (CAD), or may direct a prototyping system such as a Computer Numerically Controlled (CNC) milling machine for headform fabrication. Furthermore, by scanning subjects in various states of encumberment, it is now possible to see "through" the protective equipment to directly observe the person-equipment interface. Figure 3 is an example of two scans, encumbered and unencumbered, aligned to reveal fit quality. Designers of helmets and helmet-mounted equipment can now see the three-dimensional relationships between anatomical features and the equipment item of interest. The focus of this report is to document these relationships for a population of USAF flyers wearing the HGU-55/P helmet.
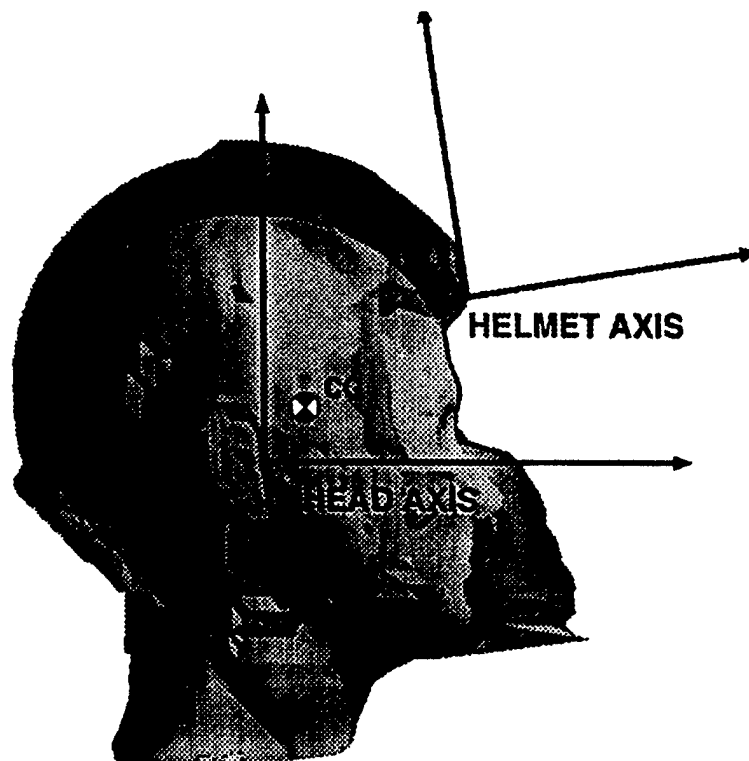
Figure 3

Illustration of subject with and without the helmet

2.0 SURVEY

2.1 Specific Aims

Initially, this survey was conducted primarily to compare the anthropometry of Air Force and Navy aviators with the anthropometry data collected in the 1988 U.S. Army anthropometric survey (ANSUR). The groups were compared by matching the aviators to the Army population for age, race, sex, height, and weight. One of the project goals was to determine the appropriateness of applying data from the larger Army anthropometric data base to Air Force and Navy anthropometric challenges. The survey plan called for data collection on 500 Air Force and 500 Navy aviators, including 50 females, 50 Blacks, 50 Hispanics, and 50 with other racial designations during the survey. The intention was to measure only pilots and Navy flight officers from the Navy and only Class I and II aviators from the Air Force.

Additionally, a Cyberware scanner was acquired to collect 3-D anthropometric data of the head and face. This would provide the opportunity to develop a database of USAF flyers defining head size and shape as well as the relationships between the head and helmet. These image data were used to generate HGU-55/P feature envelopes. Three-dimensional data were collected using the Cyberware scanner at the beginning of the Air Force portion of the survey.

2.2 Population Description

Data were collected on 365 subjects at four Air Force bases: Ellsworth AFB, South Dakota; Randolph AFB, Texas; Eglin AFB, Florida; and Hurlbert Field, Florida. Table 1 shows the survey sample size.

Table 1
1990 Air Force survey sample size

	Total sample	Pilots and navigators
Males	353	308
Females	12	8
Total	365	316

The samples for females and racial/ethnic minorities (shown in Table 2) were unfortunately, much smaller than expected. The survey plan called for an over-sampling of these groups beyond their actual proportions in the Air Force.

Table 2
Racial/ethnic composition of the 1990 Air Force survey sample

	Total sample		Pilots and navigators	
	Male	Female	Male	Female
White	343	11	300	7
Black	5	0	3	0
Hispanic	1	1	1	1
Asian/Pacific Islands	2	0	2	0
Mixed	2	0	2	0
Total	353	12	308	8

Table 3 compares the age distribution for the survey males and females (a predominantly white sample) with the population age distribution of white Air Force pilots from 1988.

Table 3
Age distribution in five year increments of the 1990 Air Force survey sample compared with ages of 1988 white pilots

| | Total sample | | Pilots and navigators | | 1988 white pilots |
	N	%	N	%	%
			Males		
<25	74	21.0	57	18.5	9.4
26-30	135	38.2	128	41.6	30.0
31-35	86	24.4	76	24.7	17.8
36-40	37	10.5	30	9.7	19.2
41-45	19	5.4	15	4.9	17.6
46-50	2	0.6	2	0.6	4.9
>50	0	0.0	0	0.0	1.1
	353	100.1	308	100.0	100.0
			Females		
<25	6	50.0	3	37.5	23.3
26-30	4	33.3	3	37.5	46.7
31-35	2	16.7	2	25.0	29.2
36-40	0	0.0	0	0.0	0.8
	12	100.0	8	100.0	100.0

Compared to the 1988 pilot population, males 35 years of age and under in the 1990 survey are over-represented while those over 35 are under-represented. As shown in the table, the large number of older subjects (over 35) in the 1988 sample represents many pilots who were not on active flying status; therefore, there is little significance in the disparity between the samples. The female samples are too small for useful conclusions.

The ranks and pay grades are given in Table 4 for both males and females. Rank is highly correlated with age; therefore, it is not surprising that the distribution of ranks among pilots and navigators is similar to the age distribution for this same group.

Table 4
Distribution of ranks for the
1990 Air Force survey sample

	Pay grade	Total sample		Pilots and navigators	
		N	%	N	%
Males					
Airman	E2	2	0.6	-	-
Airman First	E3	8	2.3	-	-
Sergeant	E4	7	2.0	-	-
Staff Sergeant	E5	2	0.6	-	-
Technical Sergeant	E6	6	1.7	-	-
Master Sergeant	E7	2	0.6	-	-
Second Lieutenant	O1	56	15.9	55	17.9
First Lieutenant	O2	39	11.0	38	12.3
Captain	O3	168	47.6	158	51.3
Major	O4	42	11.9	37	12.0
Lieutenant Colonel	O5	<u>21</u>	<u>5.9</u>	<u>20</u>	<u>6.5</u>
		353	100.0	308	100.0
Females					
Airman	E2	2	16.7	-	-
Airman First	E3	1	8.3	-	-
First Lieutenant	O1	2	16.7	2	25.0
Captain	O3	<u>7</u>	<u>58.3</u>	<u>6</u>	<u>75.0</u>
		12	100.0	8	100.0

Air Force Specialty Codes (AFSC) were recorded for each subject. These codes were used in conjunction with the subject's ranks to derive the "Abbreviated Specialties" in Table 5.

Table 5
Abbreviated Air Force specialty classification

	Male		Female	
	N	%	N	%
Fighter Pilot	76	21.5	-	-
Helicopter Pilot	11	3.1	1	8.3
Command Post Pilot	15	4.2	1	8.3
Tanker Pilot	21	5.9	-	-
Bomber Pilot	23	6.5	-	-
Other and Unknown Pilot	16	4.5	-	-
Trainer Pilot	99	28.0	3	25.0
Navigator	47	13.3	3	25.0
*Other Officers	16	4.5	1	8.3
**Enlisted	27	7.6	3	25.0
Unknown	2	0.6	-	-
	353	99.7	12	99.9

*   Composed of Command Post personnel (some or all non-rated) with intelligence or communications specialties

** Flight Crew personnel (boom operators, communications specialists)

Unlike the Navy, the Air Force does not have anthropometric constraints for individual types of aircraft. Thus, the Air Force's anthropometric selection criteria pertain to all Air Force aviators regardless of the type of aircraft flown. In principle, it was expected that aviators of one command would be anthropometrically similar to those of another command. To prevent any inadvertent bias, it was essential to sample aviators from a wide range of aircraft types. The Air Force bases selected for measuring subjects were chosen partly to provide this diversity of aircraft types. Table 6 shows the types of aircraft currently flown by all the male subjects in the 1990 survey, and the types of aircraft in which they have the most experience. The same information is provided for male pilots and navigators in Table 7 and for females in Table 8 and Table 9.

Table 6
Aircraft currently flown by 1990 USAF survey subjects
and aircraft in which they are most experienced
(total male sample)

Aircraft	Aircraft currently flying		Aircraft flown most experienced	
	N	%	N	%
ATTACK				
A-10A	0	0.0	2	0.6
AC-130A,H	9	2.5	4	1.1
AV-8B	0	0.0	1	0.3
BOMBER				
B-52G	2	0.6	7	2.0
B-52H	1	0.3	11	3.1
B-1B	36	10.2	20	5.7
FIGHTER				
F-4	6	1.7	8	2.3
F-15	66	18.7	54	15.3
F-16	4	1.1	4	1.1
F-111	1	0.3	1	0.3
TRAINING				
T-37	50	14.2	48	13.6
T-38	50	14.2	63	17.8
T-43	5	1.4	4	1.1
T-33	0	0.0	1	0.3
CARGO/TRANSPORT				
C-130	0	0.0	7	2.0
C-140	0	0.0	1	0.3
C-141B	0	0.0	4	1.1
KC-135A	0	0.0	4	1.1
KC-135R	35	9.9	31	8.8
C-12	0	0.0	1	0.3
MC-130	12	3.4	7	2.0
RECONNAISSANCE				
RF-4	4	1.1	6	1.7
HELICOPTER				
UH-1	0	0.0	3	0.8
H3; HH-3E	0	0.0	2	0.6
H-60; MH-60G	9	2.5	5	1.4
HH-1H	5	1.4	4	1.1
COMMAND POST				
EC-135	55	15.6	47	13.3
EC-130H	0	0.0	2	0.6
UNKNOWN OR N/A	3	0.8	1	0.3
	353	99.9	353	100.0

12

Table 7
Aircraft currently flown by 1990 USAF survey subjects
and aircraft in which they are most experienced
(total male pilot and navigator sample)

Aircraft	Aircraft currently flying		Aircraft flown most experienced	
	N	%	N	%
ATTACK	0	0.0	2	0.6
A-10A	9	2.9	4	1.1
AC-130A,H	0	0.0	1	0.3
AV-8B				
BOMBER	2	0.6	7	2.3
B-52G	1	0.3	10	3.2
B-52H	36	11.7	20	6.5
B-1B				
FIGHTER	6	1.9	8	2.6
F-4	66	21.4	54	17.5
F-15	4	1.3	4	1.3
F-16	1	0.3	1	0.3
F-111				
TRAINING	50	16.2	48	5.6
T-37	49	15.9	61	19.8
T-38	5	1.6	4	1.3
T-43	0	0.0	1	0.3
T-33				
CARGO/TRANSPORT	0	0.0	5	1.6
C-130	0	0.0	1	0.3
C-140	0	0.0	2	0.6
C-141B	0	0.0	3	1.0
KC-135A	25	8.1	21	6.8
KC-135R	0	0.0	1	0.3
C-12	9	2.9	7	2.3
MC-130				
RECONNAISSANCE	4	1.3	6	1.9
RF-4				
HELICOPTER	0	0.0	3	1.0
UH-1	0	0.0	2	0.6
H3; HH-3E	8	2.6	4	1.3
H-60; MH-60G	5	1.6	4	1.3
HH-1H				
COMMAND POST	27	8.8	21	6.8
EC-135	0	0.0	2	0.6
EC-130H	1	0.3	1	0.3
UNKNOWN OR N/A	308	99.7	308	99.6

13

Table 8
Aircraft currently flown by 1990 USAF survey female subjects and aircraft in which they are most experienced
(total female sample)

Aircraft	Aircraft currently flying		Aircraft flown most experienced	
	N	%	N	%
TRAINING				
T-37	1	8.3	1	8.3
T-38	2	16.7	1	8.3
T-39 A/B	0	0.0	1	8.3
CARGO/TRANSPORT				
KC-135R	3	25.0	2	16.7
RECONNAISSANCE				
RC-135	0	0.0	1	8.3
HELICOPTER				
HH-1H	1	8.3	1	8.3
UNSPECIFIED	1	8.3	1	8.3
COMMAND POST				
EC-135	4	33.3	4	33.3
	12	99.9	12	99.8

Table 9
Aircraft currently flown by 1990 USAF survey female subjects and aircraft in which they are most experienced
(total female pilot and navigator sample)

Aircraft	Aircraft currently flying		Aircraft flown most experienced	
	N	%	N	%
TRAINING				
T-37	1	12.5	1	12.5
T-38	2	25.0	1	12.5
T-39 A/B			1	12.5
CARGO/TRANSPORT				
KC-135R	2	25.0	1	12.5
RECONNAISSANCE				
RC-135	0	0.0	1	12.5
HELICOPTER				
HH-1H	1	12.5	1	12.5
COMMAND POST				
EC-135	2	25.0	2	25.0
	8	100.0	8	100.0

2.3 Survey Data Collection Methods

Data collected on each aviator included demographic and biographic information, 24 traditionally measured anthropometric dimensions, and three Cyberware scans of the head and face. The demographic and biographic information and the traditionally measured anthropometric dimensions are shown on the data collection form, included in Appendix A. Appendix B provides measurement descriptions.

Procedures for the data collection process were duplicated at each base. Data were collected at four workstations. At the first station, subjects were briefed on the reasons for collecting anthropometric data on aviators, as well as on the safe use of the laser used in the Cyberware scanner. Subjects were then asked to read and sign a consent form, included in Appendix C, and fill out a brief biographical form.

At the second station, various anatomical landmarks of the head, face, and body were located by palpation or visual inspection and marked on the subjects with an eyeliner pencil. The landmarks are described in Appendix D. Some of the landmarks were used as measuring points in traditional anthropometry while others were used as reference points in the Cyberware scans (Figure 4). Additional landmarks, such as pupils, were later located by visual inspection of the scanned image. These landmarks are shown in Figure 4.

At the third station, data were collected using traditional anthropometry. This station was staffed by a measurer and a recorder. The recorder entered the data into a laptop computer as the values were called out by the measurer. The recorder checked the data for obvious errors by comparing the subject's percentile values with the percentiles from other large data bases. The recorder also assisted in measuring and positioning the subjects. After the traditional anthropometry data were collected, felt dots were placed on the subject's face to highlight the facial landmarks on the Cyberware scans.

The fourth station consisted of the Cyberware scanner. Each subject was properly positioned for the scan. Since hair absorbs much of the laser light, a skull cap which reflects the light was used to produce clearer images. The skull cap also ensured that the image produced, and hence the data points, were representative of the subject's skull rather than his or her hair. After the regular head scan was made, two additional scans were made of each subject: one with the chin raised and another with the subject wearing his or her personal HGU-55/P helmet and oxygen mask.

After the data were collected, the landmarks were identified using the CARD Laboratory's Silicon Graphics-based, in-house developed software, INTEGRATE (Burnsides,

15

Files, & Whitestone, 1996). All landmarked data sets were run through an editing procedure where each subject's head and face were displayed two-dimensionally on a computer screen. The landmark locations, indicated by the small circles produced by the felt dots, were visibly inspected, and any landmarks found to be incorrectly placed were corrected.

2.4 Summary Statistics of Survey Demographics and Anthropometry

Summary statistics for the total male sample and the male pilot and navigator sample are listed in Tables 10 and 11, respectively, and for females in Tables 12 and 13.

Table 10
Summary Statistics For The Total 1990 Air Force Male Sample
(Weight In Kilograms; All Other Dimensions In Centimeters)

	Mean	S.D.	Minimum	Maximum	N
Weight	79.87	9.26	55.5	113.0	353
Stature	178.62	6.64	161.2	196.0	353
Shoulder Circumference	118.75	5.65	103.7	139.1	353
Waist Circumference, Omph	87.10	7.03	69.5	108.2	353
Buttock Circumference	99.26	5.23	84.8	119.7	353
Sitting Height	93.32	3.37	83.0	102.8	353
Sitting Height/Helmet	97.04	3.12	89.3	105.5	254
Eye Height Sitting	80.69	3.00	72.5	91.9	353
Acromial Height, Sitting	60.78	2.80	54.2	68.6	353
Thumbtip Reach	80.79	3.87	69.0	91.5	353
Buttock-Knee Length	62.49	2.86	54.0	72.0	352
Knee Height, Sitting	55.72	2.56	48.4	64.0	353
Head Circumference	57.76	1.42	54.2	61.8	352
Bitragion-Coronal Arc	35.00	1.28	32.0	38.6	352
Bitragion-Chin Arc	32.89	1.22	29.6	36.8	352
Bitragion Submandibular Arc	31.12	1.31	27.4	35.4	352
Head Length	19.94	.65	17.9	21.7	352
Head Breadth	15.14	.50	13.7	17.0	352
Tragion-Top of Head	13.03	.65	11.3	14.9	352
Menton-Sellion Length	12.18	.63	9.9	14.2	352
Interpupillary Breadth	6.42	.38	5.3	7.2	70
Bizygomatic Breadth	14.10	.55	12.5	15.6	352
Bigonial Breadth	11.12	.72	9.2	13.2	352

Table 11
Summary Statistics For Air Force Male Pilots And Navigators
(Weight In Kilograms; All Other Dimensions In Centimeters)

	Mean	S.D.	Minimum	Maximum	N
Weight	79.77	9.38	55.5	113.0	308
Stature	178.58	6.46	61.5	196.0	308
Shoulder Circumference	118.61	5.55	105.2	134.5	308
Waist Circumference, Omph	86.87	6.95	69.5	108.2	308
Buttock Circumference	99.18	5.33	84.8	119.7	308
Sitting Height	93.29	3.25	85.0	102.8	308
Sitting Height/Helmet	96.98	3.10	90.0	105.5	227
Eye Height Sitting	80.67	2.91	73.3	90.8	308
Acromial Height, Sitting	60.68	2.70	54.8	68.3	308
Thumbtip Reach	80.71	3.86	69.0	91.5	308
Buttock-Knee Length	62.50	2.86	54.0	72.0	308
Knee Height, Sitting	55.74	2.55	48.4	64.0	308
Head Circumference	57.78	1.39	54.2	61.6	307
Bitragion-Coronal Arc	34.98	1.25	32.0	38.1	307
Bitragion-Chin Arc	32.85	1.20	29.6	36.8	307
Bitragion Submandibular Arc	31.07	1.30	27.4	35.4	307
Head Length	19.97	.63	18.4	21.6	307
Head Breadth	15.12	.50	13.9	17.0	307
Tragion-Top of Head	13.05	.64	11.3	14.9	307
Menton-Sellion Length	12.16	.64	9.9	14.2	307
Interpupillary Breadth	6.41	.38	5.6	7.2	52
Bizygomatic Breadth	14.08	.55	12.5	15.6	307
Bigonial Breadth	11.10	.72	9.2	13.2	307

Table 12
Summary Statistics For The Total 1990 Air Force Female Sample
(Weight In Kilograms; All Other Dimensions In Centimeters)

	Mean	S.D.	Minimum	Maximum	N
Weight	59.14	6.20	51.5	70.0	11
Stature	165.13	3.33	159.0	170.6	11
Shoulder Circumference	104.10	4.40	98.0	110.2	11
Waist Circumference, Omph	76.95	7.44	68.4	89.5	11
Buttock Circumference	94.82	5.04	86.7	104.4	11
Sitting Height	86.55	2.23	83.0	89.5	11
Sitting Height/Helmet	89.48	2.18	87.6	92.5	4
Eye Height Sitting	74.79	1.95	70.9	77.2	11
Acromial Height, Sitting	57.41	1.55	54.1	59.3	11
Thumbtip Reach	73.90	1.86	71.0	77.0	11
Buttock-Knee Length	58.38	2.22	55.6	62.0	11
Knee Height, Sitting	51.09	1.34	49.0	52.9	11
Head Circumference	54.39	1.32	52.2	56.8	12
Bitragion-Coronal Arc	33.31	1.04	32.2	35.0	12
Bitragion-Chin Arc	30.33	.75	29.4	31.6	12
Bitragion Submandibular Arc	28.22	1.06	26.5	29.9	12
Head Length	18.61	.61	17.5	19.9	12
Head Breadth	14.33	.45	13.6	15.2	12
Tragion-Top of Head	12.26	.63	11.5	13.4	12
Menton-Sellion Length	11.13	.49	10.5	12.1	12
Interpupillary Breadth	6.10	.36	5.5	6.5	7
Bizygomatic Breadth	13.18	.33	12.8	14.0	12
Bigonial Breadth	9.96	.47	9.4	11.0	12

Table 13
Summary Statistics For Air Force Female Pilots And Navigators
(Weight In Kilograms; All Other Dimensions In Centimeters)

	Mean	S.D.	Minimum	Maximum	N
Weight	57.43	6.25	51.5	67.5	7
Stature	165.56	2.26	162.0	168.1	7
Shoulder Circumference	102.69	4.47	98.0	109.7	7
Waist Circumference, Omph	74.66	6.96	68.4	84.5	7
Buttock Circumference	92.66	4.25	86.7	97.3	7
Sitting Height	87.20	1.80	84.3	89.5	7
Sitting Height/Helmet	89.90	2.46	87.6	92.5	3
Eye Height Sitting	75.61	1.33	73.4	77.2	7
Acromial Height, Sitting	57.56	1.25	55.4	58.9	7
Thumbtip Reach	73.87	1.88	71.0	77.0	7
Buttock-Knee Length	57.49	1.71	55.6	59.9	7
Knee Height, Sitting	51.04	1.29	49.0	52.4	7
Head Circumference	54.35	1.17	52.2	56.0	8
Bitragion-Coronal Arc	33.13	.98	32.3	34.8	8
Bitragion-Chin Arc	30.36	.83	29.4	31.6	8
Bitragion Submandibular Arc	28.06	1.15	26.5	29.8	8
Head Length	18.56	.41	17.9	19.0	8
Head Breadth	14.43	.46	13.9	15.2	8
Tragion-Top of Head	12.26	.61	11.5	13.4	8
Menton-Sellion Length	11.36	.42	10.8	12.1	8
Interpupillary Breadth	6.23	.32	5.9	6.6	3
Bizygomatic Breadth	13.16	.21	12.9	13.4	8
Bigonial Breadth	9.98	.35	9.5	10.7	8

In Table 14, the male survey pilots and navigators (1990 Aviators) are compared with the 1967 Air Force pilots. Differences between the 1990 survey aviators and the 1967 pilots are generally small when compared with the standard deviations. The 1990 survey sample is 1.19 centimeters taller and 0.2 kilograms heavier than the 1967 Air Force pilots. Few of the variables show differences large enough to be of concern.

Table 14
1990 Aviators compared with 1967 pilots
(weight in kilograms; all other dimensions in centimeters)

*means; SD in parenthesis	1990 Aviators	1967 Pilots	1990 Aviators minus 1967 Pilots
Weight	79.77* (9.38)	79.53 (9.59)	0.24
Stature	178.58 (6.46)	177.39 (6.18)	1.19
Shoulder Circumference	118.61 (5.55)	118.15 (5.78)	0.46
Waist Circumference, Omph	86.87 (6.95)	88.64 (7.18)	-1.77
Buttock Circumference	99.18 (5.33)	99.09 (5.34)	0.09
Sitting Height	93.29 (3.25)	93.10 (3.15)	0.19
Eye Height Sitting	80.67 (2.91)	80.91 (2.96)	-0.24
Acromial Height, Sitting	60.68 (2.70)	61.09 (2.79)	-0.41
Thumbtip Reach	80.71 (3.86)	80.46 (4.05)	.25
Buttock-Knee Length	62.50 (2.86)	60.56 (2.72)	1.94
Knee Height, Sitting	55.74 (2.55)	55.86 (2.49)	-0.12
Head Circumference	57.78 (1.39)	57.67 (1.41)	0.11
Bitragion-Coronal Arc	34.98 (1.25)	35.78 (1.25)	-0.80
Bitragion-Chin Arc	32.85 (1.20)	32.78 (1.20)	0.07
Bitragion Submandibular Arc	31.07 (1.30)	31.22 (1.52)	-0.15

*means; SD in parenthesis	1990 Aviators	1967 Pilots	1990 Aviators minus 1967 Pilots
Head Length	19.97 (0.63)	19.89 (0.67)	0.08
Head Breadth	15.12 (0.50)	15.66 (0.53)	-0.54
Tragion-Top of Head	13.05 (0.64)	13.42 (0.61)	-0.37
Menton-Sellion Length	12.16 (0.64)	12.07 (0.62)	0.09
Bizygomatic Breadth	14.08 (0.55)	14.30 (0.50)	-0.30
Bigonial Breadth	11.10 (0.72)	11.81 (0.66)	-0.71

The large differences in Buttock-Knee Length are due to the differences in the measuring technique between the 1990 Air Force survey and the 1967 Air Force survey. In the 1990 survey, the measurement was taken from a buttock-plate with an anthropometer, whereas a beam caliper was used in the 1967 survey. Differences in measuring techniques could also account for differences in Waist Circumference, though that conclusion is not certain. Head Breadth and Bigonial Breadth show large differences between the means relative to their standard deviations. Head Breadth is an easily repeated measurement, so the differences between the 1990 survey and the 1967 survey is not easily explained by differences in measuring technique, thus suggesting that the differences are significant. Because of the amount of soft tissue at gonion, Bigonial Breadth is a difficult measurement; however, it is safe to assume that the differences between groups are at least partly significant rather than due to variation in measuring methods. Head Breadth, Bizygomatic Breadth, and Bigonial Breadth all indicate that 1990 Air Force survey pilots and navigators have narrower heads and faces on the average than what is found among the 1967 Air Force subjects.

3.0 FEATURE ENVELOPES

3.1 History and Definition of Feature Envelopes

This section provides background and methodology for generation of feature envelopes. Feature envelopes evolved from the ability to collect 3-D geometric fit data and the need to

condense this voluminous collection of images to an effective design tool. In general terms, a feature envelope can be described as a three-dimensional volume, with respect to a particular equipment item, that encompasses a sample of given anatomical landmarks or features. For example, feature envelopes for a helmet might describe the range of pupil locations among helmet wearers, or the volume area that contains wearers' ear locations (Whitestone & Naishadham, 1996; Whitestone, 1993).

Multiple dependent variables in a helmet system must be evaluated and measured (Blackwell & Robinette, 1993; Whitestone & Robinette, 1997). An example is optical placement to accommodate range of pupil locations versus shift in center of gravity location of the combined head/helmet configuration. As adjustments are added or expanded to allow positioning of the optics over the pupils, weight is consequently added to the helmet system. This additional weight on the front of the helmet not only moves the combined head-helmet center of gravity forward, but also increases the mass moment of inertia about the Y-axis (i.e., nodding axis). To avoid serious design flaws, designers must identify parts and functions of the system that influence or are influenced by other parts and functions. Designers also need specific definitions of the end user population to make informed decisions regarding design trade-offs.

In addition to clearly defined user populations and appropriate surface information on the user populations, the relationship between the helmet and head must be examined. A number of factors affect the orientation of the head within the helmet. Studies of head-to-helmet relationships for existing helmets provide guidance for adding additional capability to these helmets and for the development of future helmet designs.

Feature envelopes can alleviate problems associated with measurement dependence on the Frankfurt plane and the limitations of percentiles. Feature envelopes describe the spatial location and orientation of areas of interest (i.e., features) with respect to a well-defined, easily duplicated coordinate system. For a given helmet system, this definition could include the range of pupil location along the three coordinate axes, or the volume which contains the aggregate of all ears for a given population. These anthropometric design envelopes defined for an existing helmet are based on one criteria--the relationship of the head to the helmet. Helmet systems do not fit the human head in exactly the same way across a sample of people. Figure 5 shows two subjects wearing the same helmet.
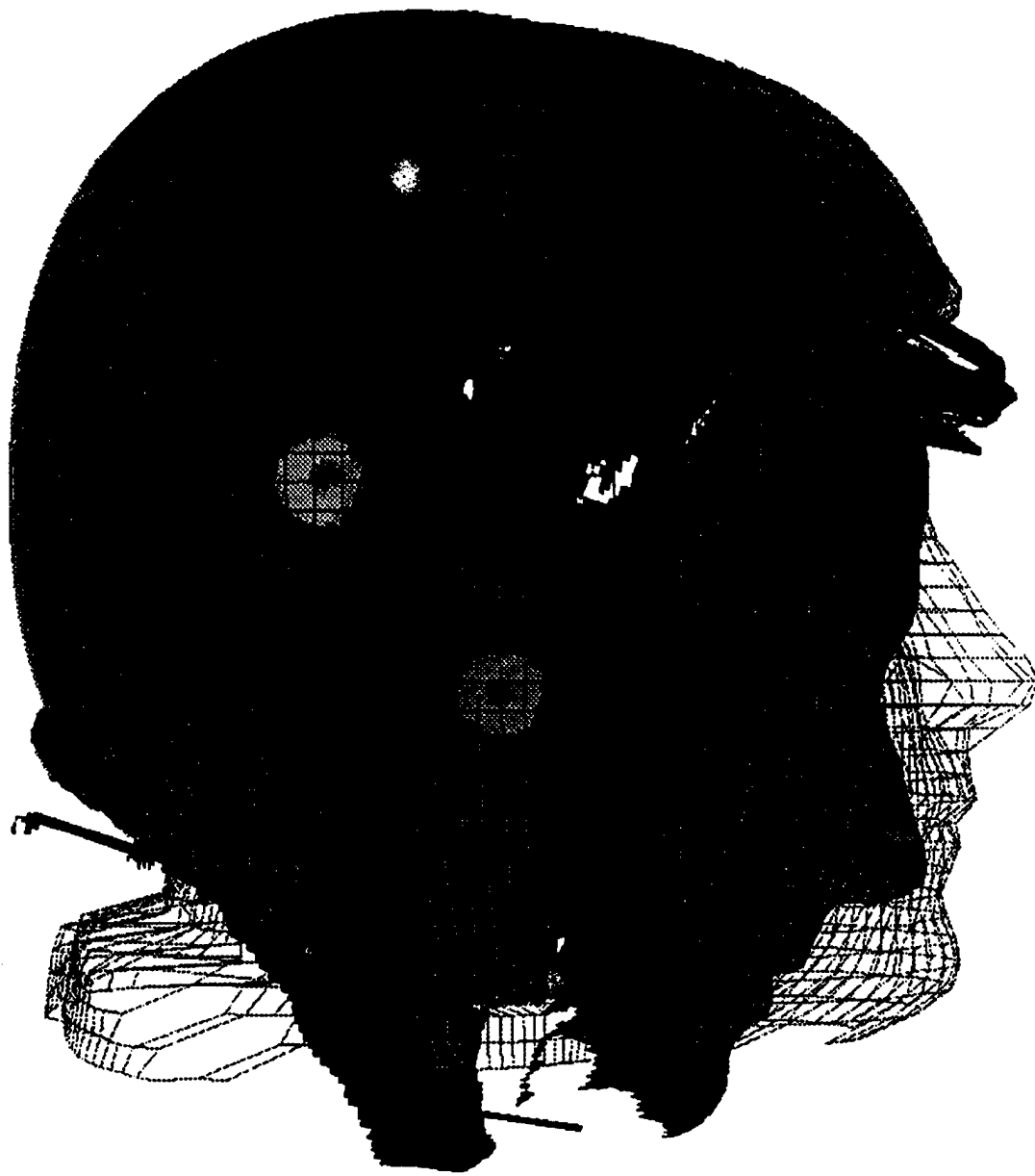
Figure 5

Two subjects wearing the HGU-55P

The orientation of the head with respect to the helmet system is entirely dependent upon the shape of the helmet, the liner system, and the added capabilities, such as optics or earcups. All of these components must be fit optimally to the individual, and as a result, the helmet system rests

on the head in a slightly different manner for everyone. To study these anthropometric design issues, accurate, high-resolution surface data is required. As equipment items are fit more closely to the human body, designers need precise pictures of the surface geometries of both the subject and the equipment. These precise pictures allow designers to examine the heart of the matter: the interface or definition of fit. A variety of surface scanning technologies and image processing tools create the precise pictures for this technique.

The development of feature envelopes was driven by a vendor-supported project to improve the fit of earphones. The objective of this project was to address the design concerns associated with the development of earphones for an existing helmet system. To fully understand the design concerns, researchers had to define the distribution of ear locations found within the helmet system. Although three helmet sizes were available (medium, large, and extra-large), the distribution of the ear points was determined for the size medium helmet, that being the worst case design problem (i.e., the largest distribution in the smallest helmet). Eleven subjects were measured and scanned in the medium helmet.

Each subject was scanned encumbered (with the helmet and mask) and unencumbered (without the helmet and the mask), and the coordinates of 41 anatomical landmarks were determined for each subject. (Again, the anatomical landmarks are used to indicate the location of underlying bony structure, such as the ends of bones, or facial features, such as pupils. See Appendix D.) Because the mask and the helmet hide many of the landmarks in the helmeted scan, the right and left ectocanthus and glabella were used to align the encumbered and unencumbered scans. The specific methodology used to register the two images is described in Section 3.2. From the unencumbered scan, the left and right tragions and ear points--additional points located on the top, back, and bottom of the ears--were selected. Ear length, ear breadth, ear-to-ear breadth, and bitragion breadth were calculated from these points for both the left and right ears of each subject.

Using helmet midline points (the front of the edge roll, the back of the edge roll, and a midline point), the data set containing landmarks from both the unencumbered and the encumbered scans was transformed into the helmet-based axis system. The origin of this coordinate system was the front of the helmet edge roll, the y-axis from this point to the back of the edge roll (midline), the x-axis perpendicular to this axis through the midline of the helmet, and the z-axis normal to both. The resulting distribution of the right and left tragions with respect to the helmet axis system can be seen in Figure 6. Figure 7 shows the same plot with ear point locations to determine the size and orientation of the ears. Figure 8 illustrates the location of two of the subjects' ears within the helmet system.

In general, for development of helmet mounted systems technology using existing helmet shells as platforms, a population of representative personnel can be scanned with and without a helmet of the same size to establish a database. Assigning a coordinate system to the helmet supports a common reference to which all of the scans can be registered. In other words, all of the encumbered scans are transformed into the helmet-based coordinate system, and since the relationship between encumbered and unencumbered scans are known, the unencumbered scans are referenced to this axis system as well. Now, essentially all of the head and face data are referenced to a common frame and the orientation of their "fit" is preserved. This database can be used to derive design envelopes of features such as ear locations or pupil range with respect to a helmet-based coordinate system. This coordinate system, and the subsequent feature envelopes, can be duplicated by designers and used as a basis for building viewing devices or acoustic equipment.

While this overall survey answered the univariate needs of the vendor, it also indicated the global need for feature envelopes for existing helmet systems. By reducing the massive 3-D surface data to landmarks of interest, and by summarizing the location of these features within the helmet, the head/helmet geometries can be identified and formatted for input into design tools such as CAD.
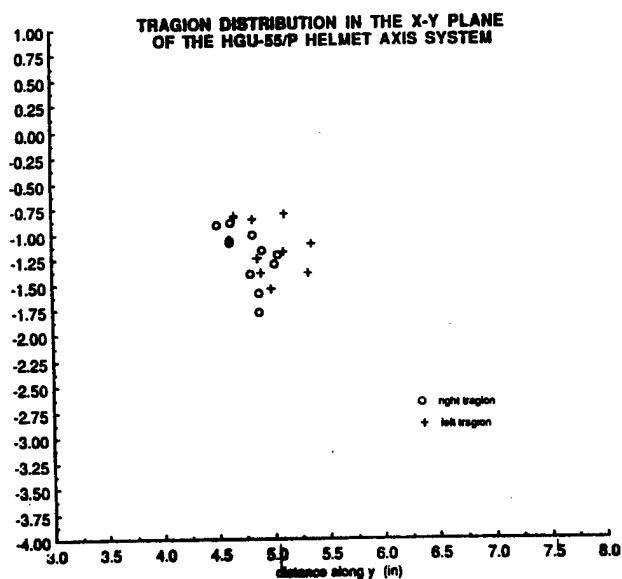
**TRAGION DISTRIBUTION IN THE X-Y PLANE
OF THE HGU-55/P HELMET AXIS SYSTEM**

Figure 6

Distribution of tragions with respect to the helmet.

**TRAGION AND EAR POINTS DISTRIBUTION
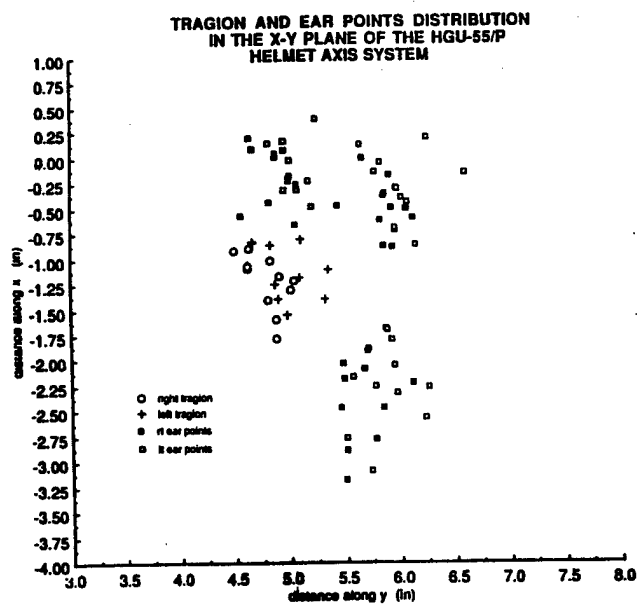IN THE X-Y PLANE OF THE HGU-55/P
HELMET AXIS SYSTEM**

Figure 7

Distribution of tragions with respect to the helmet with ear points
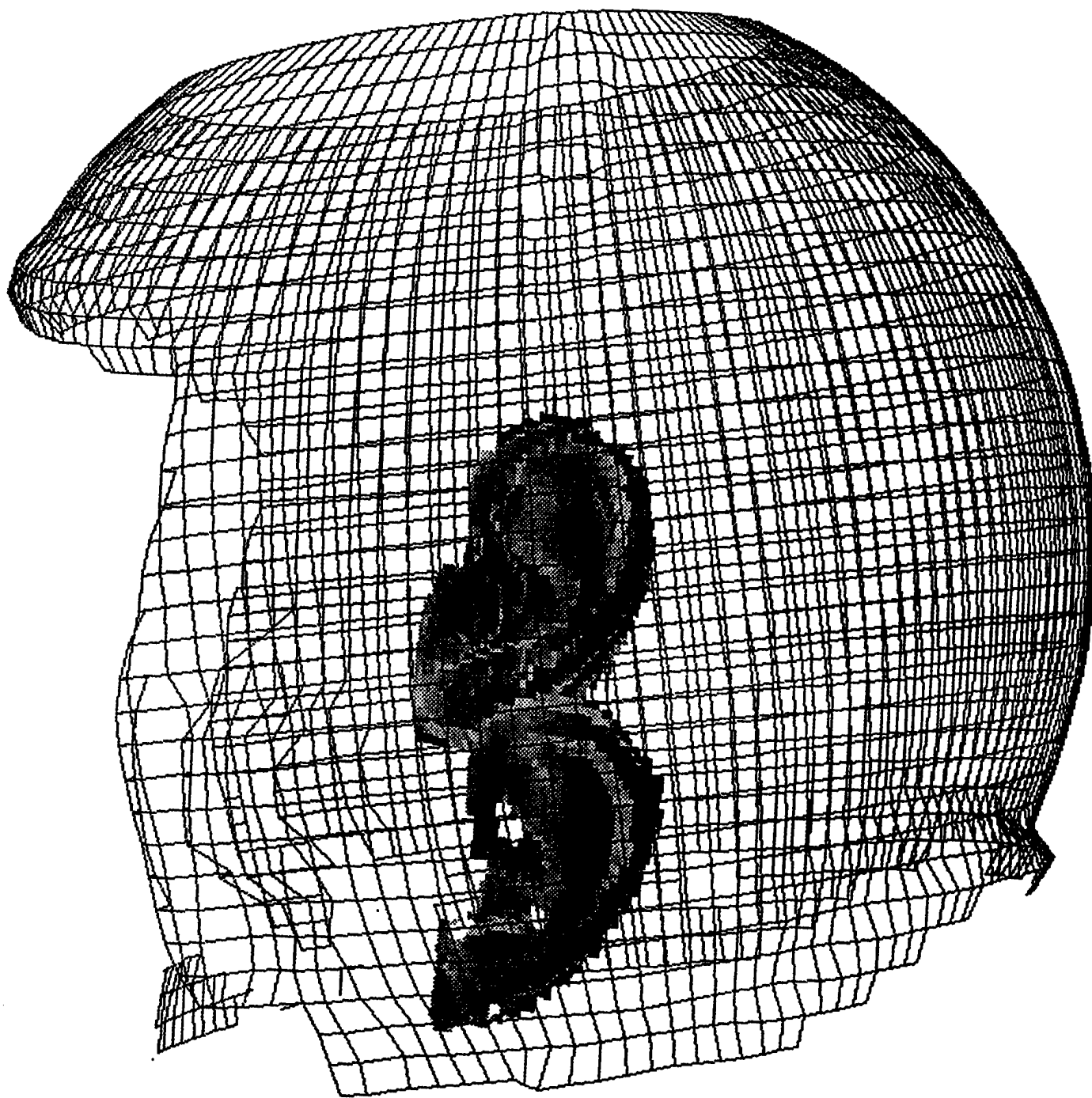
27

Figure 8

Surface data of two subjects within the helmet system

However, simply compiling the feature locations does not allow the designer to make informed decisions regarding accommodation trade-offs. Therefore, statistical summaries of these feature envelopes are needed. The statistical analyses of feature envelopes for the HGU-55/P helmet are in Appendix E.

3.2 Methodology to Develop Feature Envelopes

This section details the procedure required to establish feature envelopes for the HGU-55/P helmet system. However, this process can be used to develop feature envelopes for any equipment item. The methodology consists of:

1) landmarking the subject (and helmet) with fiducials that can be viewed in the 3-D image,

2) scanning the subject without the helmet,

3) scanning the subject with the helmet (expertly fitted),

4) scanning a representative (i.e., same helmet model, same size) helmet alone,

5) selection of all landmark coordinates using visualization software,

6) alignment of representative helmet into a helmet-based coordinate system,

7) registration of the encumbered scan with the representative helmet,

8) registration of the unencumbered and encumbered scans for each subject,

9) extraction of the landmarks or features of interest from the unencumbered scan and transformation of the coordinates into the helmet-based coordinate system,

10) generation of summary statistics of feature envelopes.

The first step required is placement of fiducials to indicate the location of landmarks. The material used in the survey to signify anatomical landmarks and reference marks on the helmet was a dark green felt sticker that, due to its low reflectivity, left a void area in the scan data. INTEGRATE, the CARD Laboratory's scan analysis software, was used to "fill in" those voids by interpolation between the neighboring points. This created pock marks in the data which could then be identified as anatomical landmarks.* It is critical to identify at least three landmarks that are visible and common to both the encumbered and unencumbered scans for registration purposes.

---

* In 1996, the CARD Laboratory purchased the Cyberware 4020 system, capable of acquiring both range data and color information on the subject. With the 4020, the landmarking process now consists of identifying color patches on the scan without relying on void areas.

The second step is to scan the subject without the helmet (unencumbered). Before the scan, subjects put on bald caps to compress their hair and to provide a reflective surface for the scanner.

In the third step, subjects put on their helmets and are scanned again. The helmets are expertly fit by Life Support technicians. However, for this survey, the helmets, although originally fit by Life Support technicians, are positioned by the pilots in the manner with which they typically wear their protective gear.

After the subjects are scanned, both with and without helmets, researchers perform the fourth step: scanning representative helmets. The representative helmets must be the same size as the helmets worn by the subjects. Felt stickers indicate reference landmarks on the representative helmets. These landmarks are used to establish a helmet-based coordinate system after the scanning is complete. In the HGU-55/P survey, dimples on the sides of the helmet and midpoints of the front and back edge rolls served as landmarks.

To complete the fifth step, data visualization software is used to identify and select landmarks in the saved scan data. For the HGU-55/P data, INTEGRATE, a software package developed by the CARD lab, was used to pick the landmark points. The coordinates of the anatomical and reference landmarks were saved in a file associated with each scan file.

Step six in the feature envelope methodology calls for aligning the representative helmet in the helmet-based coordinate system. For the HGU-55/P survey, dimples on either side of the helmet define the x-axis, positive to the left of the helmet. The z-axis runs through the midpoint of the front edgeroll and is orthogonal to x. The y-axis is orthogonal to the x and z axes (see Figure 9).
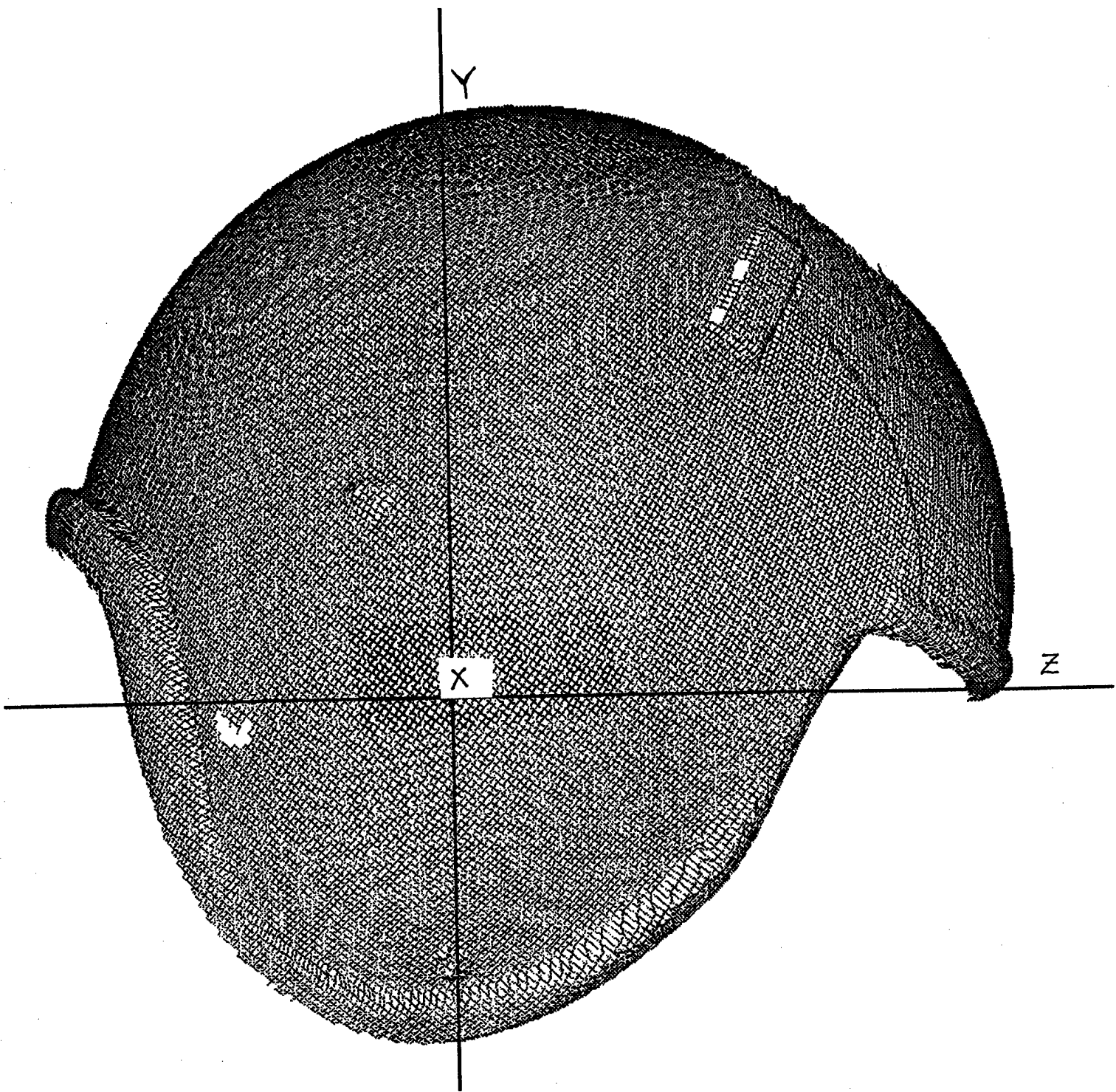
Figure 9

Axes for the helmet-based coordinate system

In step seven, each subject's encumbered scan is registered with the scan of the representative helmet. This step proved difficult in the HGU-55/P survey, because researchers did not record subjects' helmet sizes during data collection. Before the encumbered scans could be registered to representative helmets, the encumbered scans had to be examined to determine the size of each subject's helmet. Technicians compared the encumbered scans to scans of helmets of a known size, using three helmet profiles (front, top, and right). After the sizes were recorded, each encumbered scan was registered to the known-size helmet (in the helmet-based coordinate system). The transformation matrices of the alignments were saved, allowing automatic alignment in the helmet axis system from then on.

In step eight, the unencumbered scans are registered with the encumbered scans in the helmet-based axis system. Using INTEGRATE, landmarks common to both scans allow alignment of the scans automatically, using the INTEGRATE function *Iregister*, which implements a three-dimensional least squares fit of the two sets of common landmarks. The alignment accuracy can be evaluated by visually examining at the front, top, and right profiles of the aligned scans (see Figure 10). When the scans are aligned correctly, the transformation matrices from the scans are saved in an associated file to preserve the alignment. The registration process is illustrated in Figure 10.
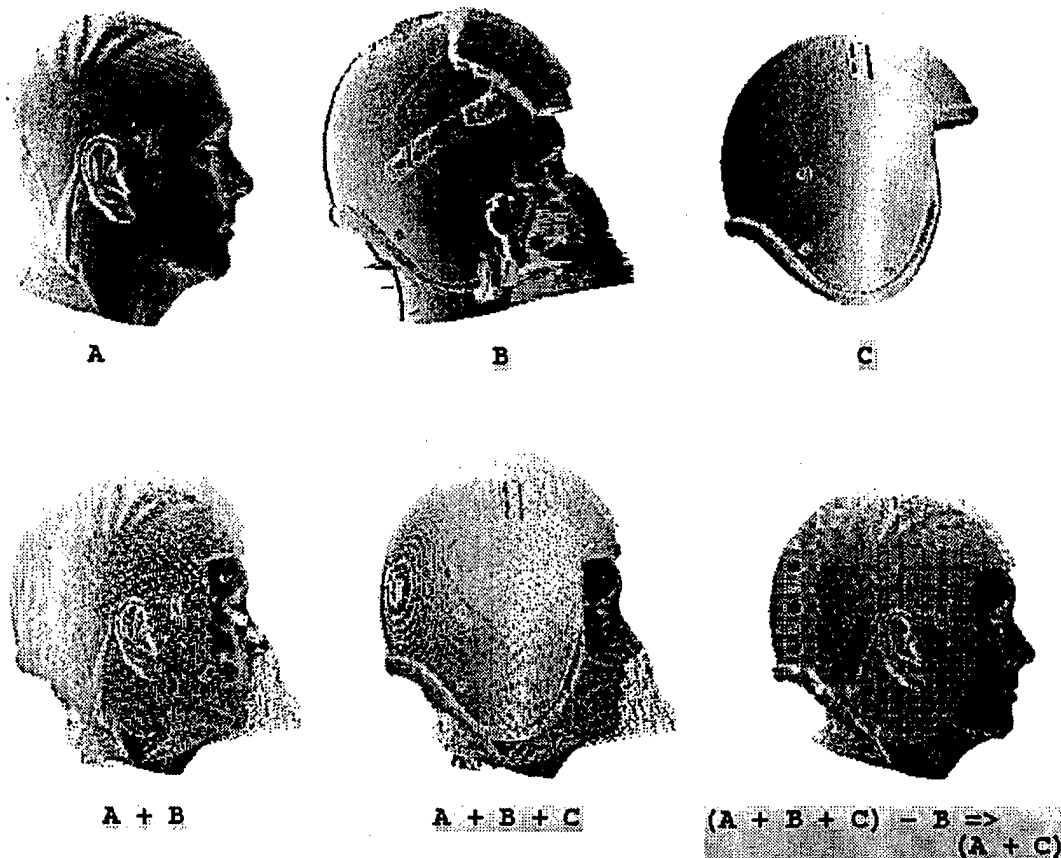
Figure 10

Helmet-to-head registration process

With the scans aligned, step nine is completed by superimposing landmark coordinates from the unencumbered scans to the representative helmet scan. The resulting pattern of landmarks shows the range of feature locations in the representative helmet. In the HGU-55/P survey, feature envelopes were created for right and left pupils, right and left tragions, and head center of gravity. (Summary statistics for Frankfurt Plane variability were also determined with respect to the helmet axis system.) Refer to Appendix D for a complete description of anatomical landmarks. Since landmarks such as pupils were unmarked landmarks during the survey, pupil position was determined by visual inspection of the scan data. If a subject's eyes were closed or the scan data were obscured due to blinking, the pupil landmark locations were estimated (Figure 11).
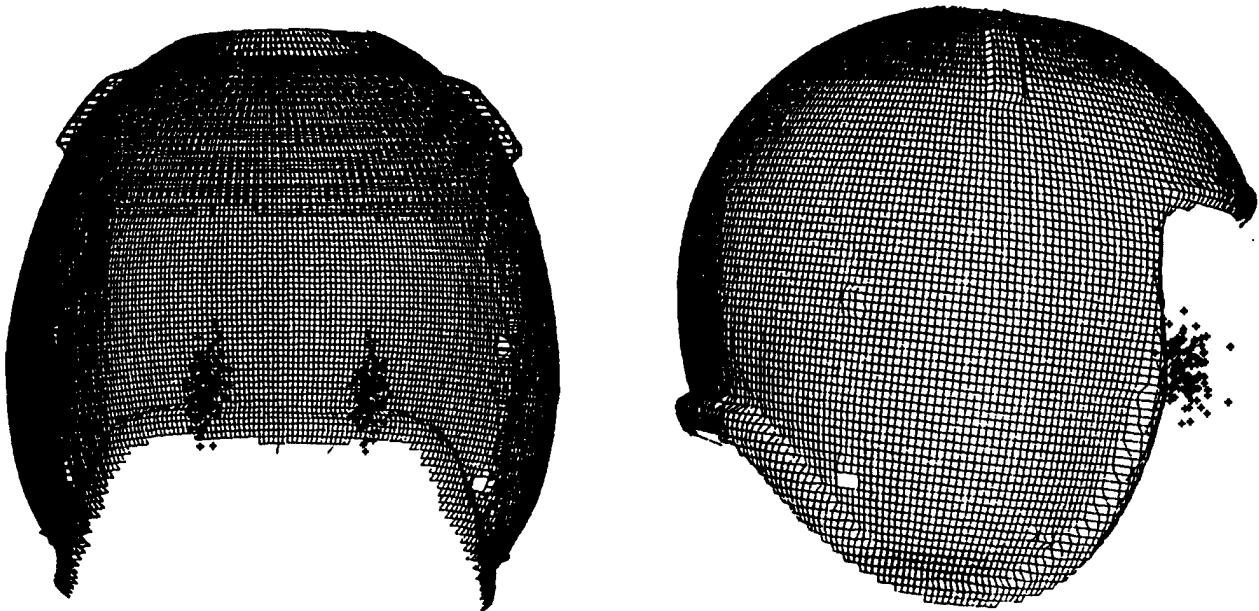
Figure 11

Pupil envelopes in a size large HGU-55/P helmet

The tragion landmarks were located by an anthropometrist during the survey, and were marked with green felt stickers. The scan landmarking technician digitized a point in the data close to the middle of the sticker (Figure 12).
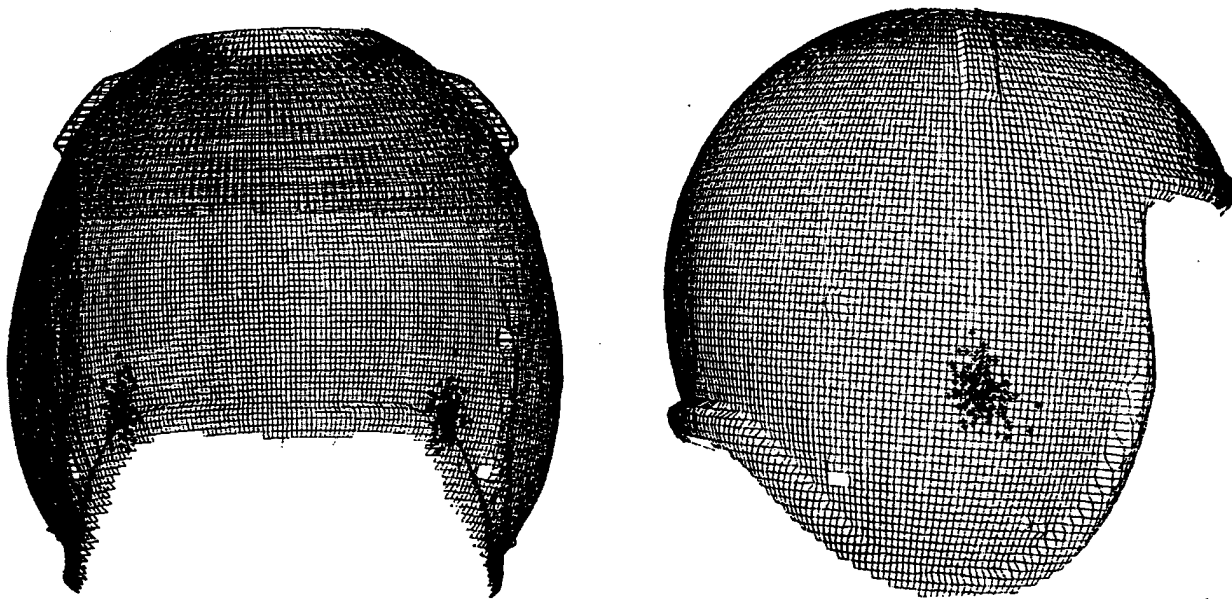
Figure 12

Tragion envelopes in a size large HGU-55/P helmet

Center of Gravity (CG) was assigned in the scan data on an individual basis using Beier's Constant (Beier, Schuller, & Schuck, 1980). Technicians aligned the scan in the anatomical axis system with the y-axis running through the left and right tragions, the x-axis running orthogonal to x, parallel to the Frankfurt Plane and in the direction of Sellion, and the z-axis orthogonal to both the x and y axes (Figure 13). With the head in the anatomical coordinate system and the origin of the head at the anatomical origin, the CG was "assigned" to the head scan in the form of an additional landmark.
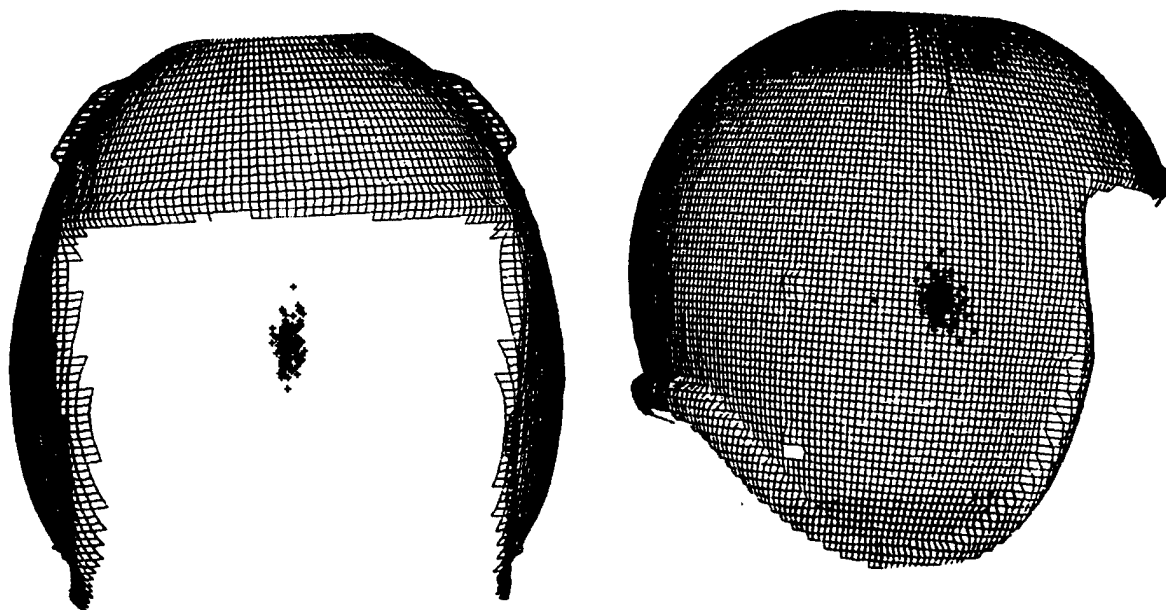
Figure 13

Head center of gravity envelope in a size large HGU-55/P helmet

4.0 RESULTS

4.1 Statistical Results for the HGU-55/P Feature Envelopes

The pupil, tragion, and center of gravity locations were analyzed in two dimensions by plotting them in the x-y, x-z, and y-z planes. However, this did not result in a comprehensive description of the three-dimensional (3-D) distribution of the data. Additionally, simply plotting them in 3-D space does not give the design enough information regarding the nature of the distribution. Instead, principal compnent analysis was used to describe the statistical representation of the data.

Principal component analysis is often used as a data reduction technique. The principal components are expressed as uncorrelated linear combinations of the original variables with maximum variance; there is one principal component for each variable. The first principal component minimizes the sum of the squared perpendicular distances from the points to the first

principal axis. Subsequent principal components maximize the next largest variations perpendicular to the previous principal components. Given that principal components are generated to maximize sample variance, a significant proportion of the entire sample variance can often be explained by a few principal components. For this application, principal component analysis is used to describe the feature envelope ellipsoid.

Principal component analysis of landmark coordinates reveals the geometric description of a multivariate normal constant density ellipsoid. This ellipsoid approximates the distribution of the landmark point cloud. The mean values for each coordinate define the center of the ellipsoid and the origin for a new axis system. The eignvectors define three orthogonal axes aligned in the direction of maximum variability in the data. The orientation of these axes also represents a helmet-to-ellipsoid rotation matrix. The semi-axis lengths of the ellipsoid are proportional to the square root of the eigenvalues. Ellipsoids of equal concentration with (1-alpha) 100% probability can be defined using a chi-square distribution with three degrees of freedom. Theoretically, the probability that any landmark in the distribution falls within a 95% probability ellipsoid is 95%.

Appendix E contains the results of the principal component analysis for each of the three sizes, medium, large, and extra-large. The summary statistics include the following for each of the landmark point clouds: cartesian coordinates for the mean location with respect to the helmet-based coordinate system, the orientation of the principal axes, and the semi-axis lengths representing ellipsoids of 95% and 99% accommodation.

Figure 14 shows the computer-aided design (CAD) files of the pupil feature envelope ellipsoids for the size large HGU-55P helmet.
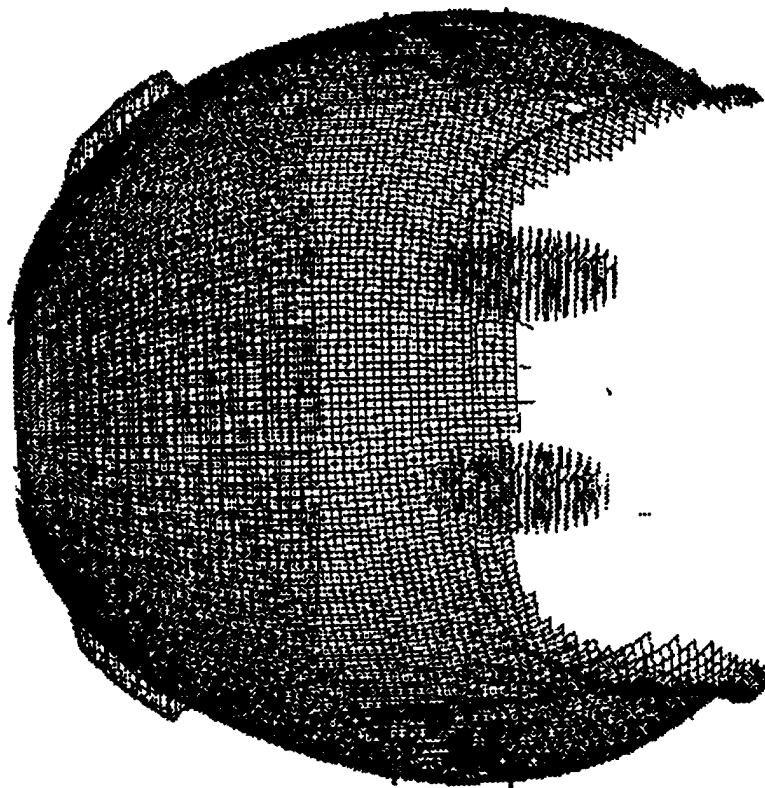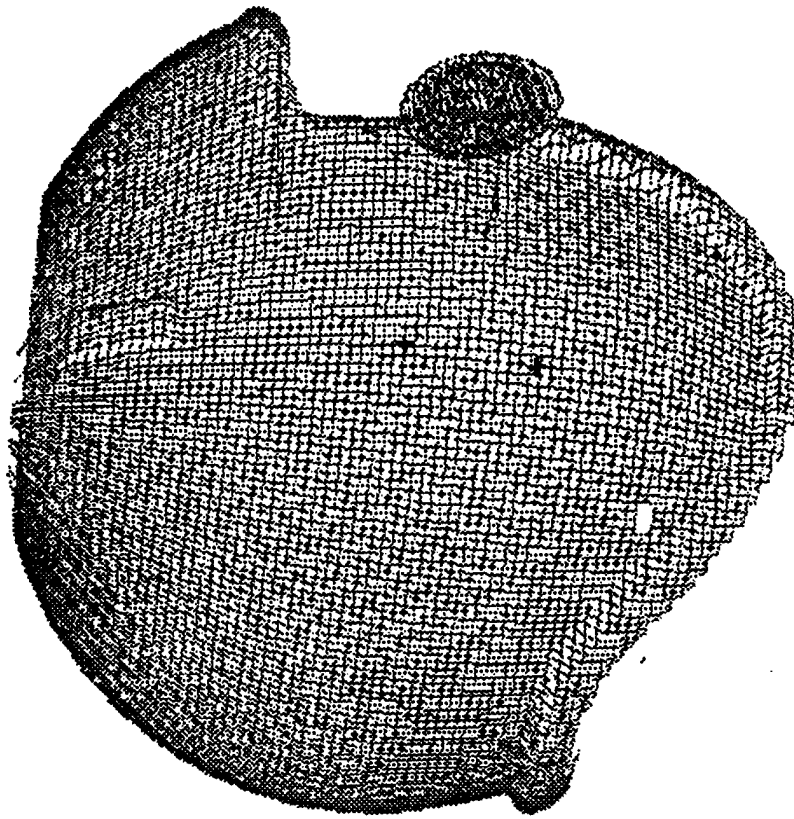
Figure 14

Pupil feature envelope ellipsoids for the size large HGU-55P helmet

The orientation of the Frankfurt plane with respect to the helmet system was also determined for each subject. The summary statistics of the angle about X of the Frankfurt plane relative to the helmet are shown in Appendix E.

4.2 Recommendation for Using Feature Envelopes

Generation of feature envelopes is intended to compress population data of subjects with existing helmet equipment into one efficient CAD file. Rather than requiring the helmet-mounted system designers to perform an exhaustive evaluation of all subject scans, a summary of the features of interest is compiled. Further, rather than report hundreds of data points representing features from hundreds of subjects for a given helmet system, ellipsoidal representations created using principal component analysis are used to further reduce and summarize the feature point clouds.

In its simplest form, a feature envelope CAD file should represent (1) the helmet size and shape of the helmet with enough definition that the designer can transfer feature envelope information to their own helmet design criteria; (2) data points or coordinates representing the location of the mean or centroid of the feature envelope point cloud; and (3) data points or coordinates representing the semi-axis lengths and locations of the principal axes for both the 95% and 99% confidence intervals.

Figure 12 illustrates the pupil and center of gravity feature envelopes for the size large HGU-55/P helmet system. A design scenario might include porting this file into a CAD system, designing a helmet-mounted display system, and virtually mounting it onto the helmet. Using the centroids of the left and right pupil envelopes, the display system adjustments are simulated to determine the ability to position the optics in front of the pupils. Depending on the accommodation requirements of the display system, the ellipsoids representing either the 95% or 99% accommodation levels are used to evaluate the adjustments on the optics.

The aircrew in this survey placed the helmets on their heads as they wear them in flight. The position of their helmets in relation to their heads did not necessarily match the Technical Order definition of fit for the HGU-55/P. Figures 15 through 18 are bivariate plots of the head length versus head breadth measurements from this flying population. The boxes overlaid on the

plots represent the definition of helmet size predicted by head dimensions according to the HGU-55/P Technical Order. Also plotted are the helmet sizes these subjects were wearing. Interestingly, the sizes worn were not always the predicted sizes. As shown in Figure 18, seven subjects, who should have worn a size large according to the T.O., wore a size medium instead. These deviations from the predicted sizes occurred among subjects predicted to wear large and extra-large helmets.

Figure 15

HGU-55/P Helmet Data: Head breadth and length measurements with size medium overlaid with helmet size boxes
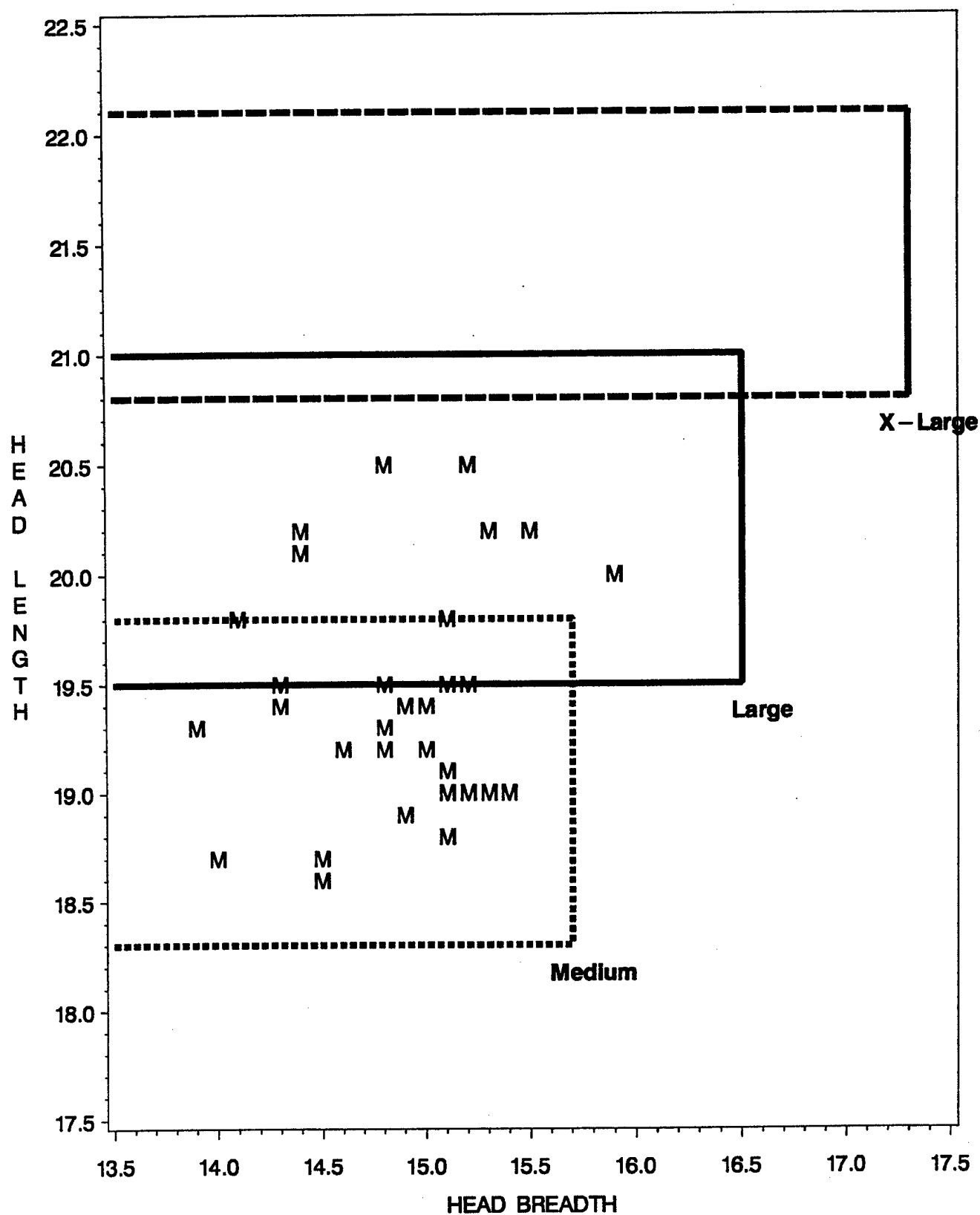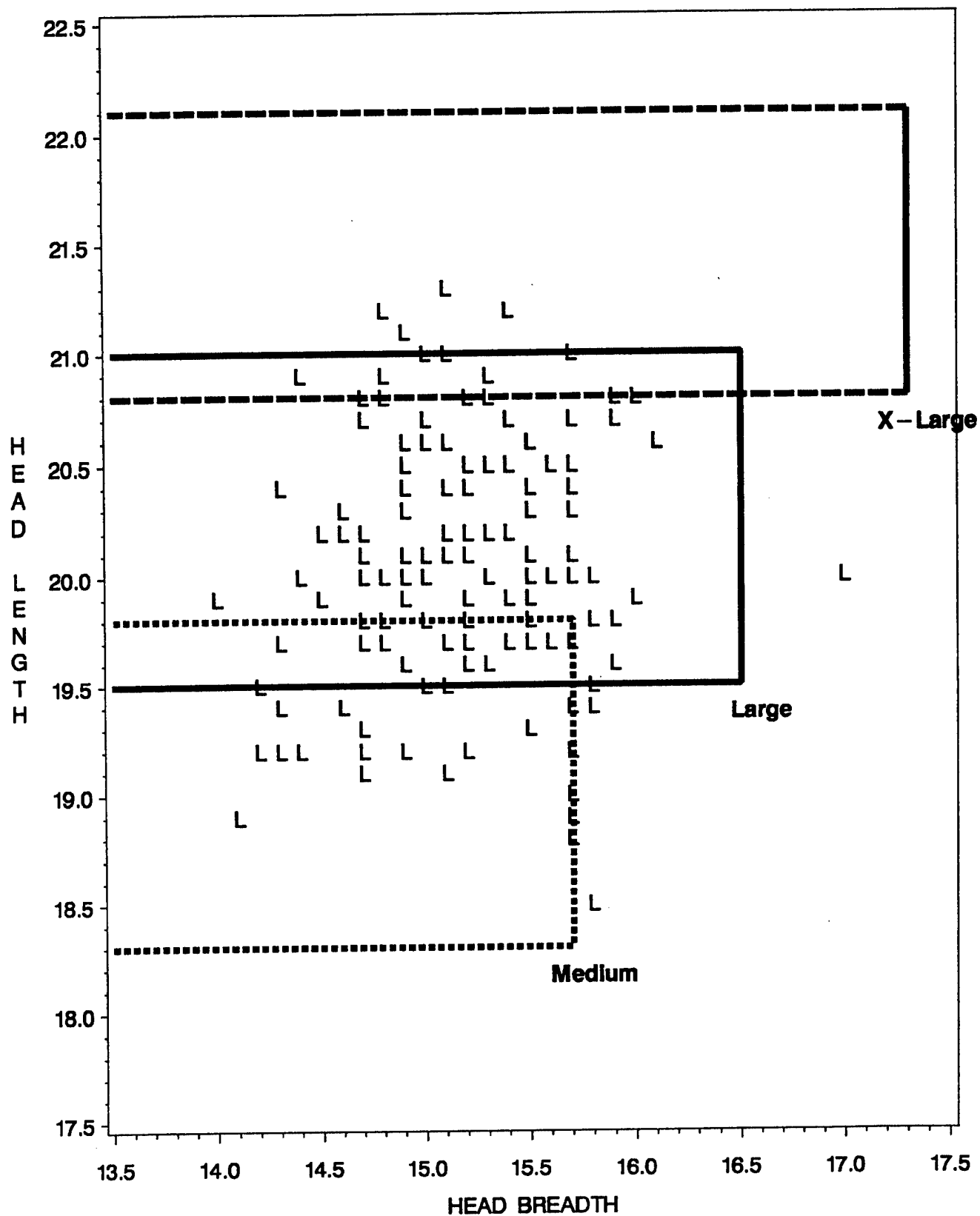
Figure 16

HGU-55/P Helmet Data: Head breadth and length measurements with size large overlaid with helmet size boxes
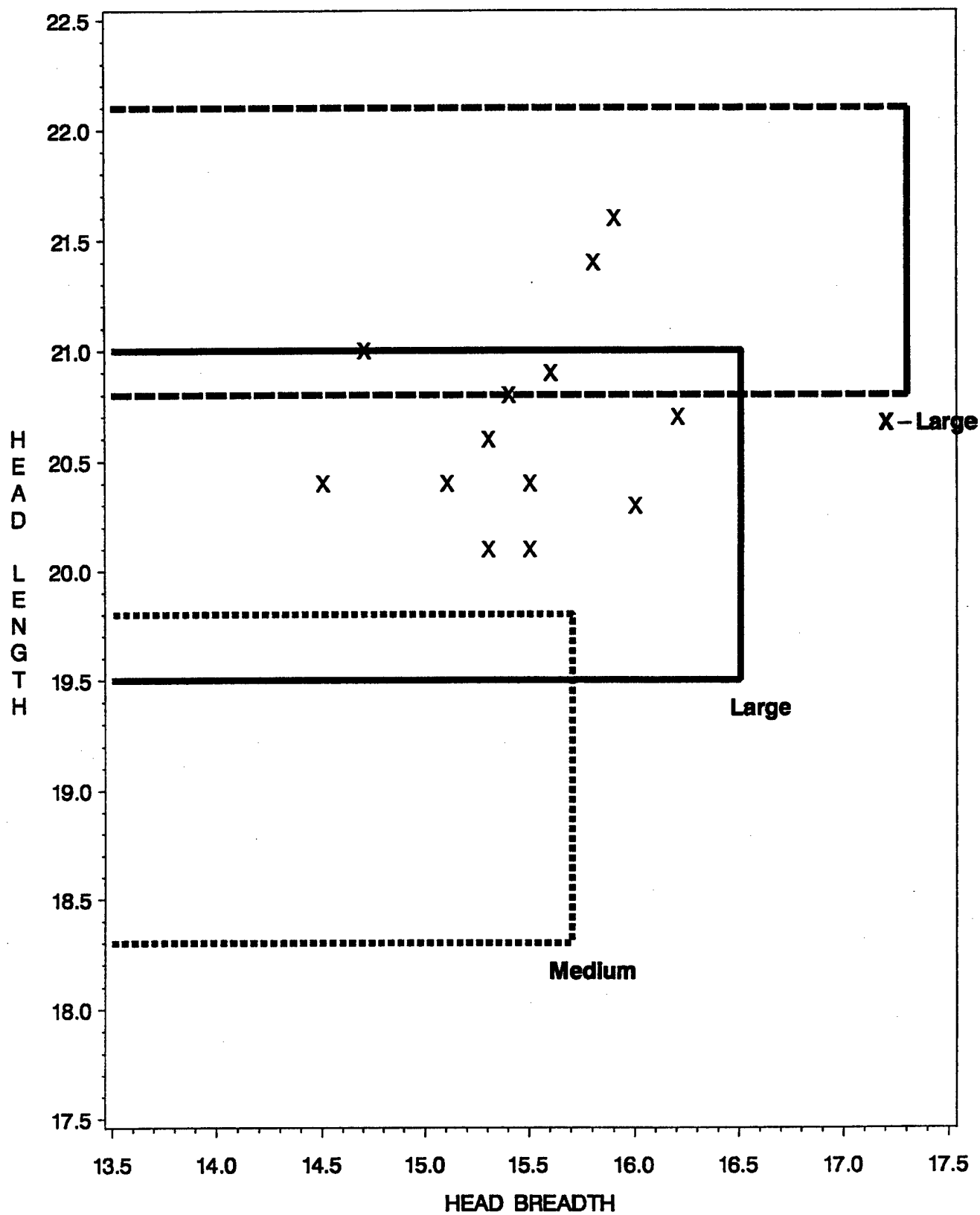
Figure 17

HGU-55/P Helmet Data: Head breadth and length measurements with size extra-large overlaid
with helmet size boxes
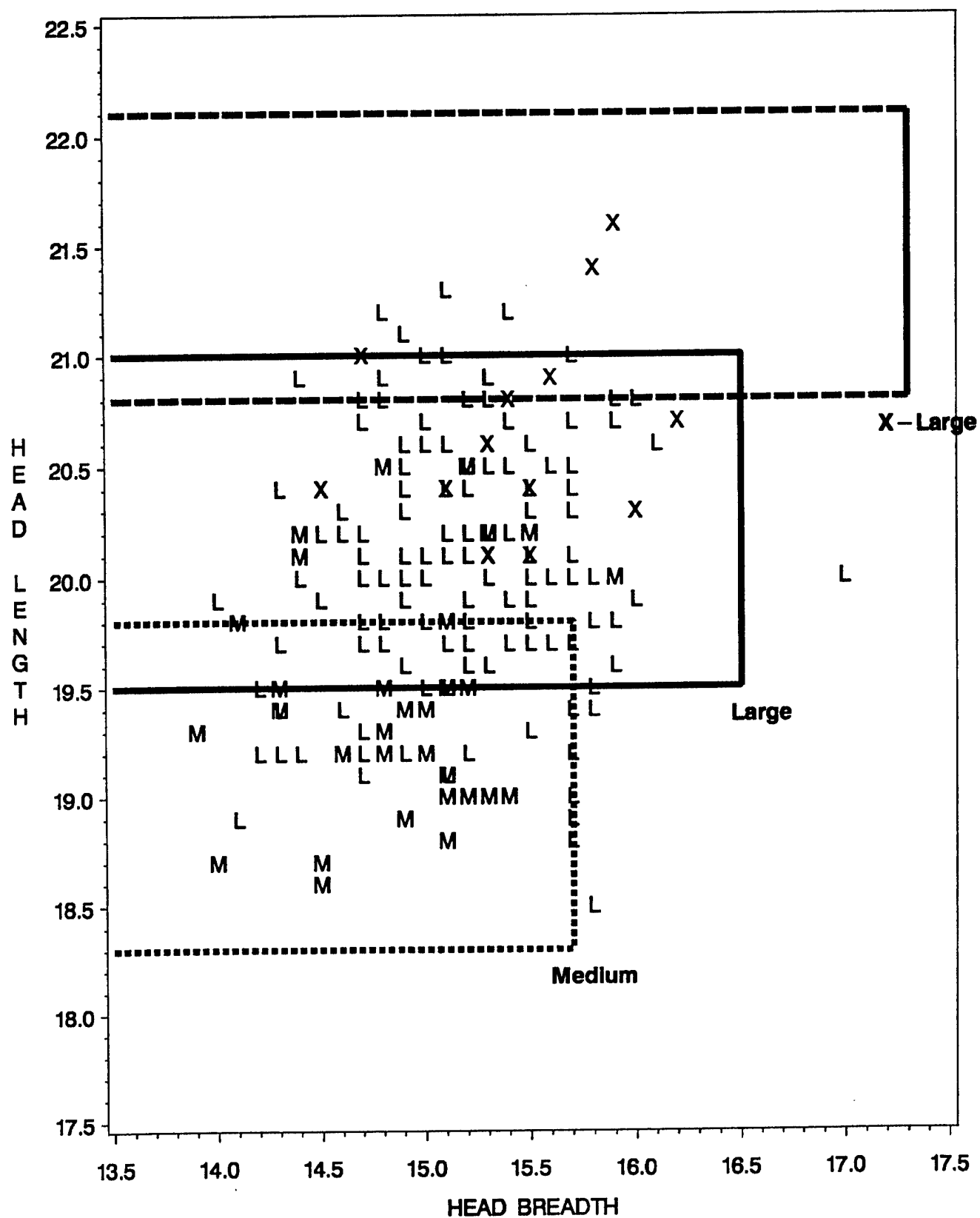
Figure 18
HGU-55/P Helmet Data: Head breadth and length measurements with helmet size overlaid with
helmet size boxes

Helmet-mounted display systems require a more precise definition of fit, so using a subset of this population data, or, in the case of feature envelopes, shorter semi-axis lengths, would be a reasonable approximation of a more restrictive helmet fit definition. Once correct placement of the HMD system has been established, the mass and center of gravity location of the HMD system with respect to the helmet-based coordinate system can be determined. Using the centroid of the CG point cloud, the estimated mass of the head (approximately 10 pounds), the mass of a helmet, and the mass of the HMD system, the newly combined CG of the head plus helmet system can be determined with respect to the helmet. For the HGU-55/P helmet system, without additional capability, the mass and center of gravity are reported for each of the three sizes (Albery ref) and are considered acceptable for safety of flight standards.

If placement of the HMD system to accommodate the targeted pupil range moves the combined CG forward of the acceptable range for safety of flight standards, then either the weight of the HMD system must be reduced or the system must be shifted backward, which could reduce accommodation. These are trade-off decisions for the helmet and HMD designers. The CG centroid in this case does not represent the worst-case subject. Additional target points, moving the CG forward and upward from the mean, should be considered during the design process.

5.0 CONCLUSION

The 1990 USAF Anthropometric Survey demonstrates that aircrew are not necessarily wearing helmets according to the specifications of associated Technical Orders; nor do the helmets sit on the head in any way specifically related to the Frankfurt plane. Feature envelopes, then, document initial locations of features for a given helmet system for a population. While these data can provide a baseline for feature location estimates it is important to note that any additional change to the helmet system, such as the addition of a helmet-mounted display, will most certainly change the position of the helmet on the head. It is imperative to include fit testing as part of the design process for helmets and helmet add-ons (Robinette, 1993; Whitestone & Robinette, 1997). A prototype system must be developed, tested, and fit, and the fit must be recorded. In this way, the changes in fit can be documented, mapped back into the CAD representation, and used to improve the design.

REFERENCES

Beier, G., Schuller, E., & Schuck, M. (1980). *Center of gravity and moments of inertia of human heads* (report in support of Office of Naval Research, contract no. N00014-75-C-0486). Munchen, Germany: Institut fur Rechtsmedizin der Universitat Munchen.

Blackwell, S.U., & Robinette, K.M. (1993). *Human integration evaluation of three helmet systems* (AL-TR-1993-0028). Human Engineering Division, Armstrong Laboratory, Wright-Patterson AFB, Ohio.

Burnsides, D.B., Files, P., & Whitestone, J.J. (1996). *INTEGRATE 1.25: A Prototype for Evaluating Three-Dimensional Visualization, Analysis, and Manipulation Functionality* (AL/CF-TR-1996-0095). Human Engineering Division, Armstrong Laboratory, Wright-Patterson AFB, Ohio.

Churchill, T., Robinette, K.M., & Potter, G. (1981). *Selected Bivariate Frequency Tables: U.S. Army Men and Women* (Natick/TR-81/012). U.S. Army Natick Research and Development Command, Natick, MA.

Hoffmeister, J.W., Pohlenz, M.Mc., Addleman, D.A., Kasic, M.A., & Robinette, K.M. (1996). *Functional Description of the Cyberware Color 3-D Digitizer 4020 RGB/PS-D* (AL/CF-TR-1996-0069). Human Engineering Division, Armstrong Laboratory, Wright-Patterson AFB, Ohio.

Hudson, J.A., Zehner, G.F., & Meindl, R.S. (1998). The USAF multivariate accommodation method. *Proceedings of the Human Factors and Ergonomics Society 42nd Annual Meeting*, 722-726.

Robinette, K.M. (1993). Fit testing as a helmet development tool. *Proceedings of the 37th Annual Meeting of the Human Factors and Ergonomics Society, 1*, 63.

Whitestone, J.J. (1993). Design and evaluation of helmet systems using 3D data. *Proceedings of the 37th Annual Meeting of the Human Factors and Ergonomics Society, 1*, 64-68.

Whitestone, J.J., & Naishadham, D. (1996). Feature Envelopes for the HGU-55/P Helmet. *Proceedings of the Thirty-fourth Annual Symposium, SAFE Association*, 12-19.

Whitestone, J.J., & Robinette, K.M. (1997). Fitting to maximize performance of HMD systems. In J. Melzer & K. Moffitt (Eds.), *Head Mounted Displays: Designing for the User* (pp. 175-202). New York: McGraw Hill.

Appendix A: Air Force Minisurvey Data Form

Subject Number _____ Date _____ Base _____

Name _____

       (Last)   (First)   (Middle)

Age _____   Birthdate ____ / ____ / ____

                          mo.   day   yr.

Air Force Specialty Code (AFSC) _____

Type of Aircraft Currently Flying _____

Type of Aircraft Most Experienced _____

Sex _____ (1) Male

      _____ (2) Female

Race   _____ (1) White, not of Hispanic Origin

         _____ (2) Black, not of Hispanic Origin

         _____ (3) Hispanic

         _____ (4) Asian/Pacific Islander

         _____ (5) American Indian/Alaskan Native

         _____ (6) Mixed (Specify) _____

         _____ (7) Other (Specify) _____

Your Birthplace _____

DO NOT WRITE BELOW THIS LINE

1.	Weight	_____
2.	Thumbtip Reach	_____
		_____
		_____
3.	Stature	_____
4.	Shoulder Circumference	_____
5.	Waist Circumference	_____
6.	Buttock Circumference	_____
7.	Head Circumference	_____
8.	Bitragion-Coronal Arc	_____
9.	Bitragion-Chin Arc	_____
10.	Bitragion-Submandibular Arc	_____
11.	Menton-Sellion Length	_____
12.	Bizygomatic Breadth	_____
13.	Bigonial Breadth	_____
14.	Head Breadth	_____
15.	Head Length	_____
16.	Tragion-Top of Head	_____
17.	Sitting Height	_____
18.	Eye Height Sitting	_____
19.	Acromial Height, Sitting	_____

Appendix B
Measurement Descriptions

STATURE

The vertical distance from a standing surface to the top of the head is measured with an anthropometer.

SHOULDER CIRCUMFERENCE

The horizontal circumference of the shoulders at the level of the maximum protrusion of the right deltoid muscle is measured with a tape.

WAIST CIRCUMFERENCE, OMPHALION

The horizontal circumference of the waist at the level of its natural indentation is measured with a tape passing over right and left waist (natural indentation) landmarks.

BUTTOCK CIRCUMFERENCE

The horizontal circumference of the trunk at the level of the maximum protrusion of the right buttock is measured with a tape.

WEIGHT

The weight of the subject is taken to the nearest tenth of a kilogram. The subject stands on the platform of a scale.

THUMBTIP REACH

The horizontal distance from a back wall to the tip of the right thumb is measured on a wall scale.

SITTING HEIGHT

The vertical distance between a sitting surface and the top of the head is measured with an anthropometer.

EYE HEIGHT, SITTING

The vertical distance between a sitting surface and the ectocanthus landmark on the outer corner of the right eye is measured with an anthropometer.

ACROMIAL HEIGHT, SITTING

The vertical distance between a sitting surface and the acromion landmark on the tip of the right shoulder is measured with an anthropometer.

KNEE HEIGHT, SITTING

The vertical distance between a footrest surface and the suprapatella landmark at the top of the right knee (located and drawn while the subject stands) is measured with an anthropometer.

48

BUTTOCK-KNEE LENGTH

The horizontal distance between a buttock plate at the most posterior point on either buttock and the anterior point of the right knee is measured with an anthropometer.

TRAGION-TOP OF HEAD

The vertical distance between the tragion landmark on the cartilaginous flap front of the earhole and the horizontal plane tangent to the top of the head is measured.

HEAD CIRCUMFERENCE

The maximum circumference of the head above the attachment of the ears to the head is measured with a tape passing just above the ridges of the eyebrows and around the back of the head.

BITRAGION-CORONAL ARC

The surface distance between the right and left tragion landmarks across the submandibular landmark at the juncture of the jaw and the neck is measured with a tape.

BITRAGION SUBMANDIBULAR ARC

The surface between the right and left tragion landmarks across the submandibular landmark at the juncture of the jaw and the neck is measured with a tape.

HEAD LENGTH

The distance from the glabella landmark between the browridges to the posterior point of the back of the head is measured with a spreading caliper.

HEAD BREADTH

The maximum horizontal breadth of the head above the attachment of the ears is measured with a spreading caliper.

BIZYGOMATIC BREADTH

The maximum horizontal breadth of the face (between the zygomatic arches) is measured with a spreading caliper.

BIGONIAL BREADTH

The straight-line distance between the right and left gonion landmarks in the corners of the jaw is measured.

MENTON-SELLION LENGTH

The straight-line distance between the menton landmark at the bottom of the chin and the sellion landmark on the deepest point of the root of the nose is measured.

49

BITRAGION CHIN ARC

The surface distance between the right and left tragion landmarks across the chin landmark at the tip of the chin is measured with a tape. The teeth are lightly occluded.

Appendix C
Consent Form

Protocol   #89-11 July 20 1989
INFORMATION PROTECTED BY THE PRIVACY ACT OF 1974

TITLE: ANTHROPOMETRY

1.   You are invited to participate in an experiment in which we hope to measure the body sizes and surface of individuals for use in the sizing and design of clothing and personal protective equipment or of aircraft and ground equipment crew and work stations.

2.   If you decide to participate, we will measure a number of dimensions on your body. These will describe the lengths, breadths, depths, circumferences, and surface contours of your body and its major segments. To aid in this process, measuring marks will be placed on your body with a water soluble colored pencil or gummed back stickers. These will be removed after measuring is completed. Measurements are made with several types of devices. One is a device which is similar to a yard stick called an anthropometer, a tape measure, and various types of calipers. Another is a light scanner which will project a line of light from a very low power laser onto your skin surface. This light will be moved around you and will be recorded in a video camera. We anticipate no medical risks to you in these procedures. We have measured many thousands of men and women with no adverse effects.

3.   Your confidentiality as a participant in this program will be protected. If statistical data collected during the test program is to be published in scientific literature, it will be done without identifying individual subjects.

4.   If you decide to participate, you are free to withdraw your consent and to discontinue participation at any time without prejudice to your future relations with the Harry G. Armstrong Aerospace Medical Research Laboratory. If you have any questions, please feel free to contact Kathleen Robinette, AAMRL/HEG (513) 255-8810.

5.   I _____, am participating because I want to. The decision to participate in this research study is completely voluntary on my part. No one has coerced or intimidated me into participating in this program. _____ has adequately answered any and all questions I have asked about this study, my participation, and the procedures involved, which are set forth above, which I have read. I understand that the principle investigator or a designee will be available to answer any questions concerning procedures throughout this study. I understand that if significant new findings develop during the course of this research which may related to my decision to continue participation, I will be informed. I further understand that I may withdraw this consent at any time and discontinue further participation in this study. The risks involved in this research are no greater than those involved in normal duties.

_____
                                              Signature Here

51

I understand that for my participation in this project I shall be entitled to payment as specified in the DOD Pay and Entitlements Manual or in current contracts. Or, I understand that I will not be paid for my participation in this experiment.

I understand that my participation in this study may be photographed, filmed or audio/video taped. I further understand that the scan produces a laser image which itself is a numeric photo. I consent to the use of these media for training purposes and understand that any release of records of my participation in this study may only be disclosed according to federal law, including the Federal Privacy Act, 5 5 U.S.C. 552a, and its implementing regulations. This means personal information will not be released to an unauthorized source without my permission.

I FULLY UNDERSTAND THAT I AM MAKING A DECISION WHETHER OR NOT TO PARTICIPATE. MY SIGNATURE INDICATES THAT I HAVE DECIDED TO PARTICIPATE HAVING READ THE INFORMATION PROVIDED ABOVE.

Volunteer signature and SSAN_____ Date _____

Witness signature_____ Date_____

Principle Investigator signature_____ Date _____

INFORMATION PROTECTED BY PRIVACY ACT OF 1974

Authority 10 U.S.C. 8012, Secretary of the Air Force; powers and duties; delegated by; implemented by DOI 12-1, Office Locator.
Purpose is to request consent for participation in approved medical research studies. Disclosure is voluntary.
Routine Use Information may be disclosed for any of the blanket routine uses published by the Air Force and reprinted in AFP 12-36 and in Federal Register 52 FR 16431.

Appendix D: Landmark Descriptions

Chelion, right and left	The most lateral point of the juncture of the fleshly (mucosal) tissue of the lips with the facial skin at the corner of the mouth.
Ectocanthus, right and left	The outer corner of the eye where upper and lower eyelids meet. This is located by visual inspection during the computerized landmarking procedure.
Endocanthus, right and left	The inner corner of the eye where the upper and lower eyelids originate. This is located by visual inspection during the computerized landmarking procedure.
Frontotemporale, right and left	The point of the deepest indentation of the temporal crest from the frontal bone above the browridges. This is located by visual inspection during the computerized landmarking procedure.
Glabella	The most anterior point on the frontal bone midway between the browridges. This is located by inspection and marked before the scan.
Gonion, right and left	The lateral point of the corner of the mandible (jaw bone). This is located by palpation and marked before the scan.
Inframalar, right and left	The inferior lateral point on the zygomatic process of the maxilla. This is located by palpation and marked before the scan.
Infraorbitale, right and left	The lowest point on the anterior margin of the zygomatic arch and the vertical line passing through zygion. This is located by palpation and marked before the scan.
Menton	The lowest point on the mandible in the midsagittal plane. This is located by palpation and marked before the scan.
Inframandibular	The intersection of the inferior mandibular border and an imaginary vertical line passing through the medial point between right and left menton and gonion. This is located by instrument and palpation, and marked before the scan.
Nuchale	The lowest palpable point (among the neck muscles) on the occipital bone, located in the midsagittal plane. This is located by palpation after the subject has donned the latex cap and marked before the scan.
Promenton	The most anterior projection of the soft tissue of the chin in the madsagittal plane. This is located by visual inspection and marked before the scan.

Pupil, right and left	The center of the pupil. This landmark is located by visual inspection during the computerized landmarking procedure.
Sellion	The point of the deepest depression of the nasal bones at the top of the nose. This is located by visual inspection during the computerized landmarking procedure when the data set is turned to a right profile.
Stomion	The point of intersection of the upper and lower lip in the midsagittal plane when the mouth is closed. This is located by visual inspection during the computerized landmarking procedure.
Submandibular	The point in the midsaggital plane where the lower jaw joins the neck. This is located by visual inspection during the computerized landmarking procedure when the data set is turned to show the right profile.
Subnasale	The point of intersection of the groove of the upper lip (the philtrum) with the inferior surface of the nose in the midsagittal plane. This is located by visual inspection during the computerized landmarking procedure when the data set is turned to a right profile.
Supraectocanthus, right and left	The protruding point of the browridge on the same vertical axis as ectocanthus. This landmark is located by visual inspection during the computerized landmarking procedure.
Supraendocanthus, right and left	The most protruding point on the browridge on the same vertical axis as right endocanthus (inside the corner of the eye). This landmark is located by visual inspection during the computerized landmarking procedure.
Suprapupil, right and left	The most protruding point on the browridge on the same vertical axis at the pupil. This landmark is located by visual inspection during the computerized landmarking procedure.
Tragion, right and left	The superior point on the juncture of the cartilaginous flap of skin (the tragus) of the ear with the head. This is located by palpation and marked before the scan.
Zygion, right and left	The most lateral point on the zygomatic arch. It is located by palpation and instrument, and marked before the scan.
Zygofrontale, right and left	The most lateral point of the frontal bone where it forms the upper margin of the bony eye socket. This is located by palpation and marked before the scan.

Appendix E
Statistical Analysis on
Feature Envelope Data

Researchers plotted and analyzed the data in two dimensions by studying it in the xy, xz, and yz planes. This did not give an appropriate presentation of the data.

To check if the data was an elliptic paraboloid, researchers studied residual plots in three dimensions using the two models $r=\theta$ and $r=\varnothing$ (in the spherical coordinate system). The residual plots of both of these models clearly indicated that the data was not a paraboloid. Observing the data on a Silicon Graphics workstation indicated the data was ellipsoidal.

To achieve a fit of the data, the 95% and 99% confidence ellipsoids were found. Principal Components Analysis was used (Tables E1, E2, and E3).

Table E-1
Principal component analysis
helmet size medium

Landmark: Right Pupil
Observations: 38
Variables: 3

Simple Statistics

	$\underline{x}$	$\underline{y}$	$\underline{z}$
Mean	-99.00736842	-8.35052632	5.223684211
Std	5.49515791	11.05802728	3.915182797

Covariance Matrix

	$\underline{x}$	$\underline{y}$	$\underline{z}$
x	30.1967605	2.0828420	-8.0631046
y	2.0828420	122.2799673	5.6460804
z	-8.0631046	5.6460804	15.3286563

Total Variance   167.80538407

Eigenvalues of the Covariance Matrix

	Eigenvalue (λ_i)	Difference	Proportion	Cumulative
PRIN1 (e_1)	122.607	88.8786	0.730650	0.73065
PRIN2 (e_2)	33.728	22.2586	0.200997	0.93165
PRIN3 (e_3)	11.470		0.068352	1.00000

Eigenvectors

	e_1	e_2	e_3
x	0.018039	0.916356	0.399957
y	0.998526	0.003972	-.054136
z	0.051197	-.400344	0.914934

56

Landmark: Left Pupil
Observations: 38
Variables: 3

Simple Statistics

	x̲	y̲	z̲
Mean	33.74789474	-44.35684211	84.95631579
Std	3.30726568	10.22262253	6.83058243

Covariance Matrix

	x̲	y̲	z̲
x	10.9380063	0.2717041	-1.5990458
y	0.2717041	104.5020114	35.8303038
z	-1.5990458	35.8303038	46.6568563

Total Variance	162.9687397

Eigenvalues of the Covariance Matrix

	Eigenvalue (λ_i)	Difference	Proportion	Cumulative
PRIN1 (e_1)	121.628	91.9658	0.750343	0.75034
PRIN2 (e_2)	29.662	18.8561	0.182992	0.93333
PRIN3 (e_3)	10.806		0.066666	1.00000

Eigenvectors

	e_1	e_2	e_3
x	-.004016	-.083012	0.996540
y	0.902213	-.430087	-.032191
z	0.431271	0.898963	0.076621

Landmark: Right Tragion
Observations: 38
Variables: 3

Simple Statistics

	$\underline{x}$	$\underline{y}$	$\underline{z}$
Mean	-72.47842105	-13.27552632	11.13921053
Std	3.12445760	7.72849193	6.57833930

Covariance Matrix

	$\underline{x}$	$\underline{y}$	$\underline{z}$
x	9.76223528	0.66442788	-6.58542304
y	0.66442788	59.72958755	18.96399552
z	-6.58542304	18.96399552	43.27454801

Total Variance	112.76637084

Eigenvalues of the Covariance Matrix

	Eigenvalue (λ_i)	Difference	Proportion	Cumulative
PRIN1 (e_1)	72.3253	39.9845	0.641373	0.64137
PRIN2 (e_2)	32.3408	24.2406	0.286795	0.92817
PRIN3 (e_3)	8.1002		0.071832	1.00000

Eigenvectors

	e_1	e_2	e_3
x	-.049466	-.249159	0.967199
y	0.831181	-.547215	-.098458
z	0.553798	0.799047	0.234164

Landmark: Left Tragion
Observations: 38
Variables: 3

Simple Statistics

	$\underline{x}$	$\underline{y}$	$\underline{z}$
Mean	72.03657895	-12.78315789	8.940526316
Std	3.58193914	7.23042599	6.424892447

Covariance Matrix

	$\underline{x}$	$\underline{y}$	$\underline{z}$
x	12.83028798	3.40135647	2.92433158
y	3.40135647	52.27906003	10.51858819
z	2.92433158	10.51858819	41.27924296

Total Variance   106.38859097

Eigenvalues of the Covariance Matrix

	Eigenvalue (λ_i)	Difference	Proportion	Cumulative
PRIN1 (e_1)	59.0724	24.1390	0.555251	0.55525
PRIN2 (e_2)	34.9333	22.5504	0.328356	0.88361
PRIN3 (e_3)	12.3829		0.116393	1.00000

Eigenvectors

	e_1	e_2	e_3
x	0.095287	0.032236	0.994928
y	0.849976	-.522863	-.064463
z	0.518133	0.851807	-.077222

Landmark: CG
Observations: 38
Variables: 3

Simple Statistics

	$\underline{x}$	$\underline{y}$	$\underline{z}$
Mean	1.593157895	10.08605263	33.76710526
Std	2.926247579	7.01821936	6.30759727

Covariance Matrix

	$\underline{x}$	$\underline{y}$	$\underline{z}$
x	8.56292489	-6.14850071	-2.03650953
y	-6.14850071	49.25540292	10.55855043
z	-2.03650953	10.55855043	39.78578329

Total Variance   97.604111095

Eigenvalues of the Covariance Matrix

	Eigenvalue (λ_i)	Difference	Proportion	Cumulative
PRIN1 (e_1)	56.9067	23.8560	0.583036	0.58304
PRIN2 (e_2)	33.0507	25.4041	0.338620	0.92166
PRIN3 (e_3)	7.6467		0.078344	1.00000

Eigenvectors

	e_1	e_2	e_3
x	-.128863	0.062192	0.989710
y	0.837138	-0.528187	0.142189
z	0.531595	0.846847	0.016001

Table E-2
Principal Component Anlaysis
Helmet Size Large

Landmark: Right Pupil
Observations: 152
Variables:3

Simple Statistics

	x	y	z
	$\underline{x}$	$\underline{y}$	$\underline{z}$
Mean	-30.23868421	-42.32381579	88.75907895
Std	3.72037253	8.12367670	6.00441343

Covariance Matrix

	x	y	z
	$\underline{x}$	$\underline{y}$	$\underline{z}$
x	13.84117177	6.65147194	2.27639394
y	6.65147194	65.99412309	17.78844348
z	2.27639394	17.78844348	36.05298060

Total Variance   115.88827546

Eigenvalues of the Covariance Matrix

	Eigenvalue (λ_i)	Difference	Proportion	Cumulative
PRIN1 (e_1)	75.0715	47.2609	0.647792	0.64779
PRIN2 (e_2)	27.8106	14.8045	0.239978	0.88777
PRIN3 (e_3)	13.0061		0.112230	1.00000

Eigenvectors

	e_1	e_2	e_3
x	0.113457	-.049389	0.992315
y	0.901512	-.414693	-.123715
z	0.417616	0.908620	-.002525

Landmark: Left Pupil
Observations: 152
Variables:3

Simple Statistics

	$\underline{x}$	$\underline{y}$	$\underline{z}$
Mean	33.84243421	-41.54519737	87.42914474
Std	3.28123018	8.09513933	6.28883263

Covariance Matrix

	$\underline{x}$	$\underline{y}$	$\underline{z}$
x	10.76647152	4.72833790	1.66182395
y	4.72833790	65.53128076	14.53150215
z	1.66182395	14.53150215	39.54941582

Total Variance	115.84716809

Eigenvalues of the Covariance Matrix

	Eigenvalue (λ_i)	Difference	Proportion	Cumulative
PRIN1 (e_1)	72.4367	39.3806	0.625278	0.62528
PRIN2 (e_2)	33.0561	22.7016	0.285342	0.91062
PRIN3 (e_3)	10.3544		0.089380	1.00000

Eigenvectors

	e_1	e_2	e_3
x	0.080733	-.018049	0.996572
y	0.910187	-.406182	-.081091
z	0.406253	0.913614	-.016364

Landmark: Right Tragion
Observations: 152
Variables: 3

Simple Statistics

	$\underline{x}$	$\underline{y}$	$\underline{z}$
Mean	-74.38690789	-9.510460526	10.86953947
Std	3.69619891	7.878224944	5.70158957

Covariance Matrix

	$\underline{x}$	$\underline{y}$	$\underline{z}$
x	13.66188640	0.96543123	2.08728355
y	0.96543123	62.06642826	3.96102230
z	2.08728355	3.96102230	32.50812363

Total Variance   108.23643829

Eigenvalues of the Covariance Matrix

	Eigenvalue (λ_i)	Difference	Proportion	Cumulative
PRIN1 (e_1)	62.6190	30.4292	0.578539	0.57854
PRIN2 (e_2)	32.1898	18.7622	0.297403	0.87594
PRIN3 (e_3)	13.4276		0.124058	1.00000

Eigenvectors

	e_1	e_2	e_3
x	0.025173	0.104039	0.994255
y	0.990917	-.134019	-.011064
z	0.132098	0.985502	-.106468

Landmark: Left Tragion
Observations: 150
Variables: 3

Simple Statistics

	x	y	z
Mean	73.01230263	-8.706447368	10.05572368
Std	3.46899368	7.633561693	6.03906451

Covariance Matrix

	x	y	z
x	12.03391718	2.72429441	4.63217812
y	2.72429441	58.27126412	3.35738019
z	4.63217812	3.35738019	36.47030014

Total Variance	106.77548143

Eigenvalues of the Covariance Matrix

	Eigenvalue (λ_i)	Difference	Proportion	Cumulative
PRIN1 (e_1)	59.0242	22.3659	0.552788	0.55279
PRIN2 (e_2)	36.6583	25.5653	0.343321	0.89611
PRIN3 (e_3)	11.0930		0.103891	1.00000

Eigenvectors

	e_1	e_2	e_3
x	0.072978	0.163767	0.983796
y	0.984172	-.171552	-.044448
z	0.161493	0.971468	-.173694

Landmark: CG
Observations: 152
Variables: 3

Simple Statistics

	x	y	z
Mean	0.801200000	14.78613333	33.4325333
Std	2.903916337	7.58328361	7.36170539

Covariance Matrix

	x	y	z
x	8.43273009	3.23752011	1.11919224
y	3.23752011	57.50619032	-9.23849282
z	1.11919224	-9.23849282	54.19470629

Total Variance   120.1336267

Eigenvalues of the Covariance Matrix

	Eigenvalue (λ_i)	Difference	Proportion	Cumulative
PRIN1 (e_1)	65.2914	18.6023	0.543489	0.54349
PRIN2 (e_2)	46.6891	38.5359	0.388643	0.93213
PRIN3 (e_3)	8.1532		0.067868	1.00000

Eigenvectors

	e_1	e_2	e_3
x	0.031275	0.076184	0.996603
y	0.769691	0.634271	-.072640
z	-.637650	0.769348	-.038801

Table E-3
Principal component analysis
helmet size extra large

Landmark: Right Pupil
Observations: 14
Variables: 3

Simple Statistics

	$\underline{x}$	$\underline{y}$	$\underline{z}$
Mean	-33.05000000	-40.73357143	105.0007143
Std	2.85441898	12.48268130	5.8092121

Covariance Matrix

	$\underline{x}$	$\underline{y}$	$\underline{z}$
x	8.1477077	13.3742538	3.1890077
y	13.3742538	155.8173324	3.7805258
z	3.1890077	3.7805258	33.7469456

Total Variance   197.71198571

Eigenvalues of the Covariance Matrix

	Eigenvalue (λ_i)	Difference	Proportion	Cumulative
PRIN1 (e_1)	157.152	123.240	0.794852	0.79485
PRIN2 (e_2)	33.912	27.265	0.171524	0.96638
PRIN3 (e_3)	6.648		0.033624	1.00000

Eigenvectors

	e_1	e_2	e_3
x	0.090047	0.101261	0.990776
y	0.995397	-.041935	-.086181
z	0.032821	0.993976	-.104571

Landmark: Left Pupil
Observations: 14
Variables: 3

Simple Statistics

	x	y	z
Mean	33.21714286	-40.82857143	103.6235714
Std	3.14025827	11.41300598	6.0101409

Covariance Matrix

	x	y	z
x	9.8612220	-8.0948879	1.2355648
y	-8.0948879	130.2567055	19.5863484
z	1.2355648	19.5863484	36.1217940

Total Variance	176.23972143

Eigenvalues of the Covariance Matrix

	Eigenvalue (λ_i)	Difference	Proportion	Cumulative
PRIN1 (e_1)	134.644	102.099	0.763984	0.76398
PRIN2 (e_2)	32.545	23.496	0.184666	0.94865
PRIN3 (e_3)	9.050		0.051350	1.00000

Eigenvectors

	e_1	e_2	e_3
x	-.061596	0.119364	0.990938
y	0.979091	-.185620	0.083218
z	0.193872	0.975345	-.105435

Landmark: Right Tragion
Observations: 14
Variables: 3

Simple Statistics

	x	y	z
Mean	-78.29357143	-10.52000000	21.95500000
Std	3.28565555	8.98494810	5.80761271

Covariance Matrix

	x	y	z
x	10.79553242	-8.37461538	-10.91928846
y	-8.37461538	80.72929231	0.97390769
z	-10.91928846	0.97390769	33.72836538

Total Variance	125.25319011

Eigenvalues of the Covariance Matrix

	Eigenvalue (λ_i)	Difference	Proportion	Cumulative
PRIN1 (e_1)	81.8268	44.0912	0.653291	0.65329
PRIN2 (e_2)	37.7356	32.0449	0.301275	0.95457
PRIN3 (e_3)	5.6907		0.045434	1.00000

Eigenvectors

	e_1	e_2	e_3
x	-.124270	-.350158	0.928411
y	0.991073	-.089328	0.098966
z	0.048279	0.932422	0.358133

Landmark: Left Tragion
Observations: 14
Variables: 3

Simple Statistics

	x	y	z
Mean	72.54714286	-7.437142857	21.55500000
Std	2.68544919	8.411125808	6.61054955

Covariance Matrix

	x	y	z
x	7.21163736	8.35189341	7.58437692
y	8.35189341	70.74703736	37.15781538
z	7.58437692	37.15781538	43.69936538

Total Variance   121.65804011

Eigenvalues of the Covariance Matrix

	Eigenvalue (λ_i)	Difference	Proportion	Cumulative
PRIN1 (e_1)	98.1434	80.2970	0.806715	0.80672
PRIN2 (e_2)	17.8464	12.1781	0.146693	0.95341
PRIN3 (e_3)	5.6683		0.046592	1.00000

Eigenvectors

	e_1	e_2	e_3
x	0.122189	0.115573	0.985755
y	0.811770	-.583086	-.032260
z	0.571051	0.804148	-.165066

Landmark: CG
Observations: 14
Variables: 3

Simple Statistics

	x	y	z
Mean	-0.863571429	15.53071429	44.80142857
Std	3.489733530	8.80103881	6.30581765

Covariance Matrix

	x	y	z
x	12.17824011	10.51893352	0.14794396
y	10.51893352	77.45828407	14.63475275
z	0.14794396	14.63475275	39.76333626

Total Variance   129.39986044

Eigenvalues of the Covariance Matrix

	Eigenvalue (λ_i)	Difference	Proportion	Cumulative
PRIN1 (e_1)	83.8718	48.6973	0.648160	0.64816
PRIN2 (e_2)	35.1744	24.8208	0.271827	0.91999
PRIN3 (e_3)	10.3537		0.080013	1.00000

Eigenvectors

	e_1	e_2	e_3
x	0.138537	-.129081	0.981909
y	0.939831	-.295507	-.171447
z	0.312292	0.946580	0.080376

The equation $(x - \bar{x})S^{-1}(x - \bar{x}) = c^2$ defines the data ellipsoid in the p-dimensional

space of x. The directions of maximum variation are the principal axes of this ellipsoid.

Geometric interpretation of Principal Components Analysis states that the principal axes

of the ellipsoid are the eigenvectors and the length of each semi-major axis proportional to the

square root of the eigenvalues. The choice $c^2 = \chi_{\rho}^2(\alpha)$ for the equation $(x - \bar{x}) S^{-1}$

$(x - \bar{x})c^2$, where $\chi_{\rho}^2(\alpha)$ is the (100α)th percentile of a Chi-Square distribution with ρ degrees

of freedom, leads to contours that contain (1-α) 100% of the probability.

Specifically, the solid ellipsoid of x values satisfying $(x - \mu)^1 \Sigma^{-1}(x - \mu) \leq \chi_{\rho}^2(\alpha)$ has

probability 1-α.

Eigenvalues and eigenvectors were obtained using the SAS covariance matrix S (Tables

18, 19, 20).

Table E-4
Eigenvalues and Eigenvectors
Helmet size medium

n=38 subjects
Landmark: Right Pupil
Centroid = (-99, -8.4, 5.2)

Direction Vector	Eigenvalue (λ_i)	Variable	FULL AXIS LENGTHS 95% $\sqrt{\chi_3^2}\,(.05) = 2.795$	FULL AXIS LENGTHS 99% $\sqrt{\chi_3^2}\,(.01) = 3.37$
$e_1^1 = (.02, 1.0, .05)$	$\lambda_1 = 122.607$ $\sqrt{\lambda_1} = 11.07$	x	$61.9 \sim 62$	$74.61 \sim 75$
$e_2^1 = (.92, 0, -.40)$	$\lambda_2 = 33.728$ $\sqrt{\lambda_2} = 5.81$	y	$32.48 \sim 33$	$39.16 \sim 39$
$e_3^1 = (.40, -.05, .91)$	$\lambda_3 = 11.47$ $\sqrt{\lambda_3} = 3.39$	z	$18.95 \sim 19$ (62, 33, 19)	$22.85 \sim 23$ (75, 39, 23)

n=38 subjects
Landmark: Left Pupil
Centroid = (33.75, -44.36, 84.96)

Direction Vector	Eigenvalue (λ_i)	Variable	FULL AXIS LENGTHS 95% $\sqrt{\chi_3^2}\,(.05) = 2.795$	FULL AXIS LENGTHS 99% $\sqrt{\chi_3^2}\,(.01) = 3.37$
$e_1^1 = (0, .90, .43)$	$\lambda_1 = 121.628$ $\sqrt{\lambda_1} = 11.03$	x	$61.66 \sim 62$	$74.34 \sim 74$
$e_2^1 = (-.08, -.43, .90)$	$\lambda_2 = 29.662$ $\sqrt{\lambda_2} = 5.45$	y	$30.47 \sim 31$	$36.73 \sim 37$
$e_3^1 = (1.0, -.03, .08)$	$\lambda_3 = 10.806$ $\sqrt{\lambda_3} = 3.29$	z	$18.39 \sim 18$ (62, 31, 18)	$22.18 \sim 22$ (74, 37, 22)

n=38 subjects
Landmark: Right Tragion
Centroid = (-72.48, -13.28, 11.14)

			FULL AXIS LENGTHS	
			95%	99%
Direction Vector	Eigenvalue (λ_i)	Variable	$\sqrt{\chi_3^2}(.05) = 2.795$	$\sqrt{\chi_3^2}(.01) = 3.37$
$e_1^1 = (-0.5, .83, .55)$	$\lambda_1 = 72.3253$ $\sqrt{\lambda_1} = 8.5$	x	47.5 ~ 48	57.29 ~ 57
$e_2^1 = (-.25, -.55, .80)$	$\lambda_2 = 32.34$ $\sqrt{\lambda_2} = 5.69$	y	31.81 ~ 32	38.35 ~ 38
$e_3^1 = (.97, -.10, .23)$	$\lambda_3 = 8.1002$ $\sqrt{\lambda_3} = 2.85$	z	15.93 ~ 16 (48, 32, 16)	19.21 ~ 19 (57, 38, 19)

n=38 subjects
Landmark: Left Tragion
Centroid = (72.04, -12.78, 8.94)

			FULL AXIS LENGTHS	
			95%	99%
Direction Vector	Eigenvalue (λ_i)	Variable	$\sqrt{\chi_3^2}(.05) = 2.795$	$\sqrt{\chi_3^2}(.01) = 3.37$
$e_1^1 = (.10, .85, .52)$	$\lambda_1 = 59.0724$ $\sqrt{\lambda_1} = 7.69$	x	42.99 ~ 43	51.83 ~ 52
$e_2^1 = (.03, -.52, .85)$	$\lambda_2 = 34.9333$ $\sqrt{\lambda_2} = 5.91$	y	33.04 ~ 33	39.83 ~ 40
$e_3^1 = (1.0, -.06, .08)$	$\lambda_3 = 12.3829$ $\sqrt{\lambda_3} = 3.52$	z	19.68 ~ 20 (43, 33, 20)	23.72 ~ 24 (52, 40, 24)

n=38 subjects
Landmark: CG
Centroid = (1.6, 10.1, 33.8)

| | | | FULL AXIS LENGTHS | |
| | | | 95% | 99% |
Direction Vector	Eigenvalue (λ_i)	Variable	$\sqrt{\chi_3^2}\,(.05) = 2.795$	$\sqrt{\chi_3^2}\,(.01) = 3.37$
$e_1^1 = (-.13, .84, .53)$	$\lambda_1 = 56.9067$	x	$42.1 \sim 42$	$50.8 \sim 51$
	$\sqrt{\lambda_1} = 7.54$			
$e_2^1 = (.07, -.53, .85)$	$\lambda_2 = 33.0507$	y	$32.1 \sim 32$	$38.76 \sim 39$
	$\sqrt{\lambda_2} = 5.75$			
$e_3^1 = (.99, .14, .02)$	$\lambda_3 = 7.6467$	z	$15.48 \sim 15$	$18.67 \sim 19$
	$\sqrt{\lambda_3} = 2.77$		$(42, 32, 15)$	$(51, 39, 19)$

n=152 subjects
Landmark: Right Pupil
Centroid = (-30.24, -42.32, 88.76)

Direction Vector	Eigenvalue (λ_i)	Variable	FULL AXIS LENGTHS 95% $\sqrt{\chi_3^2}(.05) = 2.795$	99% $\sqrt{\chi_3^2}(.01) = 3.37$
$e_1^1 = (.11, .90, .42)$	$\lambda_1 = 75.0715$ $\sqrt{\lambda_1} = 8.66$	x	$48.41 \sim 48$	$58.37 \sim 58$
$e_2^1 = (-.05, -.41, .91)$	$\lambda_2 = 27.8106$ $\sqrt{\lambda_2} = 5.27$	y	$29.46 \sim 30$	$35.52 \sim 36$
$e_3^1 = (.99, -.12, 0)$	$\lambda_3 = 13.0061$ $\sqrt{\lambda_3} = 3.61$	z	$20.18 \sim 20$ $(48, 30, 20)$	$24.3 \sim 24$ $(58, 36, 24)$

n=152 subjects
Landmark: Left Pupil
Centroid = (33.84, -41.55, 87.43)

Direction Vector	Eigenvalue (λ_i)	Variable	FULL AXIS LENGTHS 95% $\sqrt{\chi_3^2}(.05) = 2.795$	99% $\sqrt{\chi_3^2}(.01) = 3.37$
$e_1^1 = (.08, .91, .41)$	$\lambda_1 = 72.4367$ $\sqrt{\lambda_1} = 8.51$	x	$47.57 \sim 48$	$57.36 \sim 57$
$e_2^1 = (-.02, -.41, .91)$	$\lambda_2 = 33.0561$ $\sqrt{\lambda_2} = 5.75$	y	$32.14 \sim 32$	$38.76 \sim 39$
$e_3^1 = (1.0, -.08, -.02)$	$\lambda_3 = 10.3544$ $\sqrt{\lambda_3} = 3.22$	z	$17.999 \sim 18$ $(48, 32, 18)$	$21.70 \sim 22$ $(57, 39, 22)$

n=152 subjects
Landmark: Right Tragion
Centroid = (-74.39, -9.51, 10.87)

| | | | FULL AXIS LENGTHS | |
| | | | 95% | 99% |
Direction Vector	Eigenvalue (λ_i)	Variable	$\sqrt{\chi_3^2}(.05) = 2.795$	$\sqrt{\chi_3^2}(.01) = 3.37$
$e_1^1 = (.03), .99, .13)$	$\lambda_1 = 62.6190$ $\sqrt{\lambda_1} = 7.91$	x	44.2 ~ 44	53.3 ~ 53
$e_2^1 = (.10, -.13, .99)$	$\lambda_2 = 32.1898$ $\sqrt{\lambda_2} = 5.67$	y	31.7 ~ 32	38.22 ~ 38
$e_3^1 = (.99, -.01, -.11)$	$\lambda_3 = 13.4276$ $\sqrt{\lambda_3} = 3.66$	z	20.46 ~ 20.5 (44, 32, 20.5)	24.67 ~ 25 (53, 38, 25)

n=152 subjects
Landmark: Left Tragion
Centroid = (73.01, -8.71, 10.06)

| | | | FULL AXIS LENGTHS | |
| | | | 95% | 99% |
Direction Vector	Eigenvalue (λ_i)	Variable	$\sqrt{\chi_3^2}(.05) = 2.795$	$\sqrt{\chi_3^2}(.01) = 3.37$
$e_1^1 = (.07, .98, .16)$	$\lambda_1 = 59.0242$ $\sqrt{\lambda_1} = 7.68$	x	42.9 ~ 43	51.76 ~ 52
$e_2^1 = (.16, -.17, .97)$	$\lambda_2 = 36.6583$ $\sqrt{\lambda_2} = 6.05$	y	33.8 ~ 34	40.8 ~ 41
$e_3^1 = (.98, -.04, -.17)$	$\lambda_3 = 11.0930$ $\sqrt{\lambda_3} = 3.33$	z	18.6 ~ 19 (43, 34, 19)	22.4 ~ 22 (52, 41, 22)

n=150 subjects
Landmark: CG
Centroid = (.80, 14.79, 33.43)

FULL AXIS LENGTHS

Direction Vector	Eigenvalue (λ_i)	Variable	95% $\sqrt{\chi_3^2(.05)} = 2.795$	99% $\sqrt{\chi_3^2(.01)} = 3.37$
$e_1^1 = (.03, .77, -.64)$	$\lambda_1 = 65.2914$ $\sqrt{\lambda_1} = 8.08$	x	$45.17 \sim 45$	$54.46 \sim 54$
$e_2^1 = (.08, .63, .77)$	$\lambda_2 = 46.6891$ $\sqrt{\lambda_2} = 6.83$	y	$38.18 \sim 38$	$46.03 \sim 46$
$e_3^1 = (1.0, -.07, -.04)$	$\lambda_3 = 8.1532$ $\sqrt{\lambda_3} = 2.86$	z	$15.99 \sim 16$ (45, 38, 16)	$19.28 \sim 19$ (54, 46, 19)

Table E-6
Eigenvalues and Eigenvectors
Helmet size extra large

n=14 subjects
Landmark: Right Pupil
Centroid = (-33.05, -40.73, 105.0)

| | | | FULL AXIS LENGTHS | |
| | | | 95% | 99% |
Direction Vector	Eigenvalue (λ_i)	Variable	$\sqrt{\chi_3^2}(.05) = 2.795$	$\sqrt{\chi_3^2}(.01) = 3.37$
$e_1^1 = (.09, 1.0, .03)$	$\lambda_1 = 157.15$ $\sqrt{\lambda_1} = 12.54$	x	70.10 ~ 70	84.52 ~ 85
$e_2^1 = (.10, -.04, .99)$	$\lambda_2 = 33.912$ $\sqrt{\lambda_2} = 5.82$	y	32.53 ~ 33	39.23 ~ 39
$e_3^1 = (.99, -.09, -.11)$	$\lambda_3 = 6.648$ $\sqrt{\lambda_3} = 2.58$	z	14.42 ~ 14 (70, 33, 14)	17.39 ~ 17 (85, 39, 17)

n=14 subjects
Landmark: Left Pupil
Centroid = (33.22, -40.83, 103.62)

| | | | FULL AXIS LENGTHS | |
| | | | 95% | 99% |
Direction Vector	Eigenvalue (λ_i)	Variable	$\sqrt{\chi_3^2}(.05) = 2.795$	$\sqrt{\chi_3^2}(.01) = 3.37$
$e_1^1 = (-.06, .98, .19)$	$\lambda_1 = 134.644$ $\sqrt{\lambda_1} = 11.6$	x	64.84 ~ 65	78.18 ~ 78
$e_2^1 = (.12, -.19, .98)$	$\lambda_2 = 32.545$ $\sqrt{\lambda_2} = 5.71$	y	31.92 ~ 32	38.49 ~ 39
$e_3^1 = (.99, .08, -.11)$	$\lambda_3 = 9.05$ $\sqrt{\lambda_3} = 3.01$	z	16.83 ~ 17 (65, 32, 17)	20.29 ~ 20 (78, 39, 20)

n=14 subjects
Landmark: Right Tragion
Centroid = (-78.29, -10.5, 22)

Direction Vector	Eigenvalue (λ_i)	Variable	FULL AXIS LENGTHS 95% $\sqrt{\chi_3^2}(.05) = 2.795$	99% $\sqrt{\chi_3^2}(.01) = 3.37$
$e_1^1 = (-.12, .99, .05)$	$\lambda_1 = 81.8268$ $\sqrt{\lambda_1} = 9.05$	x	50.6 ~ 51	60.997 ~ 61
$e_2^1 = (-.35, -.09, .93)$	$\lambda_2 = 37.7356$ $\sqrt{\lambda_2} = 6.14$	y	34.32 ~ 34	41.38 ~ 41
$e_3^1 = (.93, .10, .36)$	$\lambda_3 = 5.6907$ $\sqrt{\lambda_3} = 2.39$	z	13.36 ~ 13 (51, 34, 13)	16.11 ~ 16 (61, 41, 16)

n=14 subjects
Landmark: Left Tragion
Centroid = (72.55, -7.44, 21.6)

Direction Vector	Eigenvalue (λ_i)	Variable	FULL AXIS LENGTHS 95% $\sqrt{\chi_3^2}(.05) = 2.795$	99% $\sqrt{\chi_3^2}(.01) = 3.37$
$e_1^1 = (.12, .81, .57)$	$\lambda_1 = 98.1434$ $\sqrt{\lambda_1} = 9.91$	x	55.4 ~ 55	66.79 ~ 67
$e_2^1 = (.12, -.58, .80)$	$\lambda_2 = 17.8464$ $\sqrt{\lambda_2} = 4.22$	y	23.59 ~ 24	28.44 ~ 28
$e_3^1 = (.99, -.03, -.17)$	$\lambda_3 = 5.6683$ $\sqrt{\lambda_3} = 2.38$	z	13.30 ~ 13 (55, 24, 13)	16.04 ~ 16 (67, 28, 16)

n=14 subjects
Landmark: CG
Centroid = (-.86, 15.53, 44.8)

Direction Vector	Eigenvalue (λ_i)	Variable	FULL AXIS LENGTHS 95% $\sqrt{\chi_3^2(.05)} = 2.795$	99% $\sqrt{\chi_3^2(.01)} = 3.37$
$e_1^1 = (.14, .94, .31)$	$\lambda_1 = 83.8718$ $\sqrt{\lambda_1} = 9.16$	x	$51.2 \sim 51$	$61.74 \sim 62$
$e_2^1 = (-.13, -.3, .95)$	$\lambda_2 = 35.1744$ $\sqrt{\lambda_2} = 5.93$	y	$33.15 \sim 33$	$39.97 \sim 40$
$e_3^1 = (.98, -.17, .08)$	$\lambda_3 = 10.3537$ $\sqrt{\lambda_3} = 3.22$	z	18 $(51, 33, 18)$	$21.70 \sim 22$ $(62, 40, 22)$

The half lengths of the axes were determined by the formula $\sqrt{\chi_\rho^2(\alpha)} * \sqrt{X_j}$, $j = 1, 2, 3$. Each

axis passed through the centroid and the eigenvector corresponding to the eigenvalue.

Correlation coefficients were calculated to check if any correlation existed between the

angle of rotation in the yz plane for the pupils and the tragions (Table 21, Figure___). They

indicate a resonable degree of correlation.

Table E-7
Correlation Analysis

Simple Statistics

Variable	N	Mean	Std Dev	Sum	Minimum	Maximun
Tragion Angle	151	89.8685	0.0735	13570	89.6897	90.0298
Pupil Angle	151	89.1504	0.0347	13462	89.0693	89.2557

Pearson Correlation Coefficients

	Tragion Angle	Pupil Angle
Tragion Angle	1.00000 0.0	0.54954 0.0001
Pupil Angle	0.54954 0.0001	1.00000 0.0

A summary of the angles data is also provided in Table E-8.

Table E-8
Summary Statistics For The Angles Data

Helmet Size	Subjects	Mean of x angles	Std Dev of the Mean	Std Dev of x angles	Coefficient of Variation	Range
Medium	38	-31.1000	1.03730	6.39434	-20.5606	28.6

Univariate Procedure (variable x angle)

Moments

N	38	Sum Wgts	38
Mean	-31.1	Sum	-1181.8
Std Dev	6.394339	Variance	40.88757
Skewness	0.338419	Kurtosis	-0.09279
USS	38266.82	CSS	1512.84
CV	-20.5606	Std Mean	1.037299
T: Mean = 0	-29.9817	Pr > | T|	0.0001
Num ^ =0	38	Num > 0	0
M (Sign)	-19	Pr > = | M|	0.0001
Sgn Rank	-370.5	Pr > = | S|	0.0001

Quantiles (Def 5)

100% Max	-15.6	99%	-15.6
75% Q3	-26.4	95%	-19.4
50% Med	-31.3	90%	-21.4
25% Q1	-35.0	10%	-39.4
0% Min	-44.2	5%	-39.9
		1%	-44.2

Range	28.6
Q3-Q1	8.6
Mode	-31.3

Extremes

Lowest	Obs	Highest	Obs
-44.2	34	-22.9	35
-39.9	17	-21.4	26
39.5	30	-19.9	10
39.4	29	-19.4	38
38.7	27	-15.6	4

Helmet Size	Subjects	Mean of x angles	Std Dev of the Mean	Std Dev of x angles	Coefficient of Variation	Range
Large	152	-31.1954	0.41383	5.10209	-16.3553	25.9

Univariate Procedure (variable x angle)

Moments

N	152	Sum Wgts	152
Mean	-31.1954	Sum	-4741.7
Std Dev	5.102088	Variance	26.0313
Skewness	0.109086	Kurtosis	-0.14486
USS	151849.9	CSS	3930.727
CV	-16.3553	Std Mean	0.413834
T: Mean = 0	-75.3814	Pr > |T|	0.0001
Num ^ =0	152	Num > 0	0
M (Sign)	-76	Pr > = |M|	0.0001
Sgn Rank	-5814	Pr > = |S|	0.0001

Quantiles (Def 5)

100% Max	-15.90	99%	-19.8
75% Q3	-27.90	95%	-22.9
50% Med	-30.90	90%	-24.2
25% Q1	-34.65	10%	-38.0
0% Min	-41.80	5%	-39.8
		1%	-41.1

Range	25.90
Q3-Q1	6.75
Mode	-30.50

Extremes

Lowest	Obs	Highest	Obs
-41.8	82	-22.1	6
-41.4	131	-20.6	81
-41.4	99	-20.2	132
-41.2	74	-19.8	60
-40.9	109	-15.9	19

Helmet Size	Subjects	Mean of x angles	Std Dev of the Mean	Std Dev of x angles	Coefficient of Variation	Range
Extra Large	14	-29.4571	1.11329	4.16556	-14.1411	15.7

Univariate Procedure (variable x angle)

Moments

N	14	Sum Wgts	14
Mean	-29.4571	Sum	-412.4
Std Dev	4.165557	Variance	17.35187
Skewness	1.463259	Kurtosis	2.605494
USS	12373.7	CSS	225.5743
CV	-14.1411	Std Mean	1.113292
T: Mean = 0	-26.4595	Pr > |T|	0.0001
Num ^ =0	14	Num > 0	0
M (Sign)	-7	Pr > = |M|	0.0001
Sgn Rank	-52.5	Pr > = |S|	0.0001

Quantiles (Def 5)

100% Max	-18.6	99%	-18.6
75% Q3	-27.9	95%	-18.6
50% Med	-30.5	90%	-24.4
25% Q1	-31.3	10%	-34.0
0% Min	-34.3	5%	-34.3
		1%	-34.3

Range	15.7
Q3-Q1	3.4
Mode	-30.5

Extremes

Lowest	Obs	Highest	Obs
-34.3	8	-29.4	1
-34.0	5	-27.9	9
-33.1	6	-26.1	7
-31.3	14	-24.4	12
-31.1	3	-18.6	2